Geophysical Journal International

Geophys. J. Int. (2013) **194,** 719–736
Advance Access publication 2013 April 29

doi: 10.1093/gji/ggt131

Characterizing and minimizing the effects of noise in tide gauge time series: relative and geocentric sea level rise around Australia

Reed J. Burgette,[1,*] Christopher S. Watson,[1] John A. Church,[2] Neil J. White,[2] Paul Tregoning[3] and Richard Coleman[4]

[1]*Surveying and Spatial Science Group, School of Geography and Environmental Studies, University of Tasmania, Private Bag* 76, *Hobart, Tasmania* 7001, *Australia. E-mail: Reed.Burgette@utas.edu.au*
[2]*Centre for Australian Weather and Climate Research, A partnership between CSIRO and the Australian Bureau of Meteorology, CSIRO Marine and Atmospheric Research, GPO Box* 1538, *Hobart, Tasmania* 7001, *Australia*
[3]*Research School of Earth Sciences, The Australian National University, Canberra, ACT, Australia*
[4]*Institute for Marine and Antarctic Studies, University of Tasmania, Private Bag* 129, *Hobart, Tasmania* 7001, *Australia*

Accepted 2013 April 3. Received 2013 March 15; in original form 2012 November 16

SUMMARY

We quantify the rate of sea level rise around the Australian continent from an analysis of tide gauge and Global Positioning System (GPS) data sets. To estimate the underlying linear rates of sea level change in the presence of significant interannual and decadal variability (treated here as noise), we adopt and extend a novel network adjustment approach. We simultaneously estimate time-correlated noise as well as linear model parameters and realistic uncertainties from sea level time series at individual gauges, as well as from time-series differences computed between pairs of gauges. The noise content at individual gauges is consistent with a combination of white and time-correlated noise. We find that the noise in time series from the western coast of Australia is best described by a first-order Gauss–Markov model, whereas east coast stations generally exhibit lower levels of time-correlated noise that is better described by a power-law process. These findings suggest several decades of monthly tide gauge data are needed to reduce rate uncertainties to $<0.5\,\mathrm{mm\,yr^{-1}}$ for undifferenced single site time series with typical noise characteristics. Our subsequent adjustment strategy exploits the more precise differential rates estimated from differenced time series from pairs of tide gauges to estimate rates among the network of 43 tide gauges that passed a stability analysis. We estimate relative sea level rates over three temporal windows (1900–2011, 1966–2011 and 1993–2011), accounting for covariance between time series. The resultant adjustment reduces the rate uncertainty across individual gauges, and partially mitigates the need for century-scale time series at all sites in the network. Our adjustment reveals a spatially coherent pattern of sea level rise around the coastline, with the highest rates in northern Australia. Over the time periods beginning in 1900, 1966 and 1993, we find weighted average rates of sea level rise of 1.4 ± 0.6, 1.7 ± 0.6 and $4.6 \pm 0.8\,\mathrm{mm\,yr^{-1}}$, respectively. While the temporal pattern of the rate estimates is consistent with acceleration in sea level rise, it may not be significant, as the uncertainties for the shorter analysis periods may not capture the full range of temporal variation. Analysis of the available continuous GPS records that have been collected within 80 km of Australian tide gauges suggests that rates of vertical crustal motion are generally low, with the majority of sites showing motion statistically insignificant from zero. A notable exception is the significant component of vertical land motion that contributes to the rapid rate of relative sea level change ($>4\,\mathrm{mm\,yr^{-1}}$) at the Hillarys site in the Perth area. This corresponds to crustal subsidence that we estimate in our GPS analysis at a rate of $-3.1 \pm 0.7\,\mathrm{mm\,yr^{-1}}$, and appears linked to groundwater withdrawal. Uncertainties on the rates of

*Now at: Department of Geological Sciences, University of Oregon, Eugene, OR 97403-1272, USA.

vertical displacement at GPS sites collected over a decade are similar to what we measure in several decades of tide gauge data. Our results motivate continued observations of relative sea level using tide gauges, maintained with high-accuracy terrestrial and continuous co-located satellite-based surveying.

Key words: Time-series analysis; Sea level change; Space geodetic surveys; Global change from geodesy; Australia.

1 INTRODUCTION

Changes in sea level relative to the land have direct impacts on coastal societies. Sea level rise is of particular significance in Australia, where approximately 6 per cent of postal addresses are located within 3 km of the coast and have an elevation of less than 5 m above sea level (Chen & McAneney 2006). Accurately quantifying the rate of sea level change and its geographic pattern is also important for scientific investigations of the Earth's climate, global response to mass loading, and crustal deformation. Global mean sea level has been rising at a rate of approximately 1.7 mm yr^{-1} since 1900, as inferred from tide gauges, and 3.1–3.2 mm yr^{-1} from satellite altimetry and tide gauges since 1993 (Nerem & Mitchum 2001; Bindoff *et al.* 2007; Church & White 2011). Observed rates of global sea level rise since the early 1970s (Church *et al.* 2011) and since 1900 (Gregory *et al.* 2013) are consistent with global estimates of the components of ocean volume change, within the uncertainties in the various data sets. There is considerable variability around the globally averaged rate of sea level rise in smaller regions of the oceans (Church *et al.* 2004; Jevrejeva *et al.* 2006). In this study, we analyse the tide gauges around continental Australia to more accurately quantify the spatial variation of relative sea level change. We investigate the effects of time-correlated noise on the uncertainty in the linear rates of relative sea level change estimates for Australia, and present an adjustment method that reduces this uncertainty by taking advantage of additional information within the data set from this network of tide gauges using a technique modified from Burgette *et al.* (2009). Additionally, we analyse the records of continuous Global Positioning System (GPS) receivers nearest to tide gauges to obtain estimates of geocentric sea level rise, separating the effects of vertical land motion from observed relative sea level change. The greater detail possible in this regional study is an important complement to global studies of vertical land motion at tide gauges, (e.g. Woppelmann *et al.* 2009; Bouin & Woppelmann 2010; King *et al.* 2012; Santamaría-Gómez *et al.* 2012).

Analysis of many geophysical time series, including vertical land motion derived from space geodetic techniques as well as sea level derived from tide gauges, is complicated by the presence of time-correlated noise (Agnew 1992). In this study, we seek to resolve the linear rate of sea level rise from time series of relative sea level that include other signals with often much larger variances than the long-term sea level change signal in which we are interested. In the case of monthly sea level data, higher frequency signals such as wind waves and swell are effectively attenuated, both mechanically with stilling wells at many tide gauge installations and through data averaging. The monthly averaging also serves to attenuate tidal signals, including those at fortnightly and monthly periods. In addition to providing a simple and effective tidal filter, monthly averaging provides a consistent record for gauges that in some cases have had different frequencies of observations recorded through time. At most tide gauges, the dominant signal in a time series of monthly means is the seasonal cycle caused by periodic variations in water temperature, wind, air pressure, currents and longer period tidal signals. Similar processes produce additional signals at interannual and longer time scales.

Central to any estimation or analysis of rates of sea level rise is the partly philosophical issue of unravelling signal versus noise. Here, we have chosen to quantify the underlying signal which we hypothesize is of climatic origin and assume to be linear over the time periods considered. The longer period time-correlated noise in time series of tide gauge observations is the result of other physical climatic and oceanographic processes (and potentially non-linear vertical land motion). However, given the potential complexities and uncertainties of these processes, in this study, we treat all departures from a periodic seasonal cycle and constant rate of change of sea level as noise. An example of the potential complexities can be seen in a study of the Fort Denison tide gauge record in Sydney Harbour (Holbrook *et al.* 2011). Much of the interannual to decadal variation in the tide gauge time-series lags climate indices, such as the Southern Oscillation Index, by years. Holbrook *et al.* (2011) investigated the sea level anomalies with a deterministic model of the regional ocean and found that much of the residual signal in the record can be explained by the effects of propagating Rossby waves interacting with the East Australian Current. Therefore, given the continent-wide scope of this study, and our incomplete knowledge of the forcing mechanisms that generate the residual signals around Australia, we do not seek to quantitatively explain signals beyond a simple linear model. However, we estimate realistic uncertainties for model parameters using an analysis that explicitly investigates the nature of time-correlated noise in sea level time series.

Most studies of sea level change attempt to reduce the effects of the noise in tide gauge records by identifying and removing common mode noise that is shared temporally and spatially between gauges in the network. If there are sufficiently long tide gauge records, one can average the residuals from linear fits of a few long-duration stations to remove the common mode noise from all of the records that share the noise (e.g. Woodworth *et al.* 1999). Another approach uses principal component analysis to solve for the shared noise from multiple time series (e.g. Aubrey & Emery 1986), but this technique is best suited to records with consistent length and complete data sets. Additionally, this technique has the complication of requiring either the de-trending of the time series before the analysis or separating out the common mode trend from shared noise after the analysis. In this study, we use an alternative technique that uses the rates of many intersite differenced time series as weighted observations in a generalized least-squares adjustment to determine more accurate linear rates of sea level change for all of the tide gauges in the network (Burgette *et al.* 2009). This technique uses all of the available data within the analysed time period, and handles missing data without requiring interpolation. Significantly, for the case of Australia where the coastline borders different oceanic basins and includes both eastern and western boundary currents, our technique analyses the data from the entire coastline, taking advantage of the precise relative rates between nearby tide gauges around the

entire perimeter of the continent without requiring a single master record. We analyse our data sets over consistent temporal windows to further minimize the bias of noise in the time series for assessing spatial variations in sea level change rate.

2 NATURE OF NOISE IN TIME SERIES

The residual time-correlated noise from tide gauge records has a 'coloured' power spectrum, with greater power at lower frequencies (Fig. 1). As with other geodetic time series, the time-correlated noise in many tide gauge records appears to represent a power-law process (Agnew 1992; Mazzotti *et al.* 2008). Power-law noise is distinguished in the frequency domain by the relationship between power (P) and frequency (f),

$$P(f) = P_0 \left(f / f_0\right)^{\kappa}, \tag{1}$$

where P_0 and f_0 are normalizing constants and κ is the spectral index (Mandelbrot & Van Ness 1968). Special cases of spectral indices of 0, -1 and -2 correspond to white, flicker and random walk noise, respectively (Fig. 1). While noise generated by some geophysical processes seems to produce power-law noise with a particular integer spectral index, fractional values of κ have been inferred for other processes (e.g. Agnew 1992; Williams 2003). More negative values of the spectral index correspond to greater degrees of time correlation in the time series, with greater noise power at periods approaching the time-series length. Greater power in the lowest frequency noise consequently creates greater levels of uncertainty in estimating the trend over the length of a full record. A second noise model that we consider in our analysis of sea level

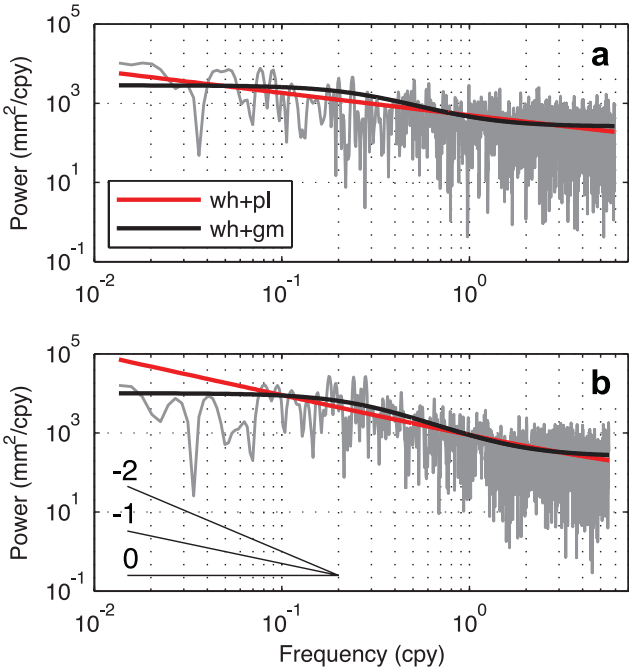

Figure 1. Power spectra of residual time series for the 1900–2011 portions of the (a) Sydney and (b) Fremantle tide gauge records. The heavy lines show best-fit noise spectra for the two candidate noise models we consider (see legend in top panel). Reference lines in lower panel show slopes in the spectral domain corresponding to integer spectral indices for white, flicker, and random walk power-law noise. Sydney is best matched by a white + power-law noise model (wh+pl), whereas the Fremantle spectrum is significantly better fit by a white + first-order Gauss–Markov model (wh+gm).

time series is first-order Gauss–Markov noise. First-order Gauss–Markov noise shows increasing power with lower frequencies as per random walk power-law noise, but at the lowest frequencies resolved in the time series (beyond a crossover frequency, f_c), the power flattens to a constant level. The power spectrum for this noise follows the relationship

$$P(f) = P_0 \left(4\pi^2 f_c^2 + 4\pi^2 f^2\right)^{-1} \tag{2}$$

(Langbein 2004; Williams & Willis 2006). For a given noise level, the trend of a time series characterized by a first-order Gauss–Markov noise model can be estimated with greater confidence than a time series characterized by a power-law noise model approaching random walk, as the noise does not interfere with the trend at the lowest frequencies.

Ordinary least-squares regression assumes that the residual noise is white, with no temporal correlation between the residuals. Consequently, determinations of linear trends from time series with time-correlated noise can underestimate the uncertainty on the rate parameter significantly (e.g. Zhang *et al.* 1997). Analyses of other time series of geodetic measurements have explicitly taken into account the effects of the spectral signature of the residual noise for over a decade, for example, in determining crustal velocities from GPS data (Langbein & Johnson 1997; Zhang *et al.* 1997). While some sea level studies have accounted for effects of serial correlation using lag-1 autocorrelation (e.g. Maul & Martin 1993; Burgette *et al.* 2009; Chambers *et al.* 2012), few sea level studies have directly investigated the effects of long-period time-correlated noise in the data, with some recent exceptions (Mazzotti *et al.* 2008; Hughes & Williams 2010). In this study, we use a maximum likelihood estimation (MLE) technique (Williams 2008) to determine linear model parameters with realistic uncertainties while simultaneously solving for the magnitude of white and coloured noise in the time series.

3 METHODS

3.1 Sea level data and analysis

Continental Australia provides a good location for an in-depth study of regional sea level change, as there have been more than 120 tide gauges in locations around an entire shoreline that borders different ocean basins. Two of the tide gauges are among the longest running in the Southern hemisphere, but the majority have much shorter durations. The regional scope of this study allows in-depth inspection of the tide gauge and GPS records, and we are able to investigate the feasibility of using shorter duration observations to add spatial density on scales that are not practical in global studies. Our approach involves first identifying a set of the highest quality tide gauge records available around Australia, adding more recent stations to the list analysed in previous studies of sea level rise around the continent (Aubrey & Emery 1986; Lambeck 2002; Church *et al.* 2006). By conducting our analysis over three time periods with sets of consistent data, we minimize effects of record length on the estimation of rates. We use the CATS software (Williams 2008) to estimate the linear rate of sea level change and the noise properties of each individual time series as well as differenced time series between pairs of relatively close tide gauges (separated by tens to hundreds of kilometres). The individual and intersite differenced rates are then used as the input to a least-squares adjustment to refine our estimates of the rate of sea level change at each tide gauge site in

the network. We outline our data selection process and adjustment theory in the following sections.

3.1.1 Sea level data selection

We analysed monthly mean relative sea level data for all tide gauges on continental Australia available from two sources. The Permanent Service for Mean Sea Level (PSMSL) archives data collected by a variety of different agencies around Australia, and includes records that extend back to the late nineteenth century at some gauges (Woodworth & Player 2003). The PSMSL sea level records have been collected for a variety of reasons, and have varying levels of quality. We initially consider both the 'metric' and 'revised local reference' (RLR) sets of PSMSL data. The other source of data is the Australian Baseline Sea Level Monitoring Project (ABSLMP; NTC 2011). The ABSLMP data are collected at a network of 15 tide gauges distributed around the Australian coastline, installed in the period 1990–1993 with the purpose of precisely monitoring sea level change. All of the ABSLMP stations are regularly monitored for vertical stability with respect to local tide gauge benchmarks using high-precision levelling (NTC 2011). We limited our analysis to tide gauges with data collected over at least the period of 1993.0–2009.0.

Although most of the data have been screened for quality in some way, we conducted a further check on the consistency of each time series by systematically differencing it with its 10 closest neighbours (Fig. 2). For this screening step, we removed a site-specific seasonal cycle (annual + semi-annual periods) from each record before forming differences to more clearly reveal the long-period intersite sea level variations. We removed sites that showed obvious steps and/or marked changes in slope relative to two or more of their neighbours (Table S1). We discarded sites rather than estimating datum changes as our detection limit changes with network density through time, and the presence of clear problems may indicate other significant, but less obvious issues. This process identified problems such as splicing records of two separated tide gauges into one time series (e.g. Bundaberg and Burnett Heads) as well as other unknown likely datum instabilities. Through this iterative process of data selection, we retained all of the ABSLMP stations, 81 per cent of the PSMSL RLR sites not included in the ABSLMP, and 26 per cent of the PSMSL metric records not redundant with the RLR. Differenced time series at 18 sites showed early or late data that differed from the trend defined by the majority of the time series, and in these cases, we have excluded the divergent months, retaining temporally contiguous data that appear to be referenced to a constant datum (Table S2). We combined the records at five tide gauge locations that had different durations in different data sources in cases where the resulting time series show a consistent trend.

Interannual variations in sea level can bias estimates of long-term rates calculated from different time periods. To capture the spatio-temporal variations of sea level change, we focus our analysis on three temporal windows with consistent data sets. Many of the current Australian tide gauges were installed in the early 1990s, and our first (and most recent) window includes all data collected from 1993.0 to 2011.0 at 43 stations. This time period coincides with the collection of satellite altimeter data beginning with the TOPEX/Poseidon mission. A number of other tide gauges began operating in the mid-1960s, and our second temporal set contains records from 1966.0 to 2011.0 at 14 stations. Our third window includes the two longest duration tide gauges from 1900.0 to 2011.0.

3.1.2 Time-series analysis

For each individual tide gauge time series, as well as intersite differenced time series, we estimate a linear model using the CATS software (Williams 2008). The model parameterises the linear rate

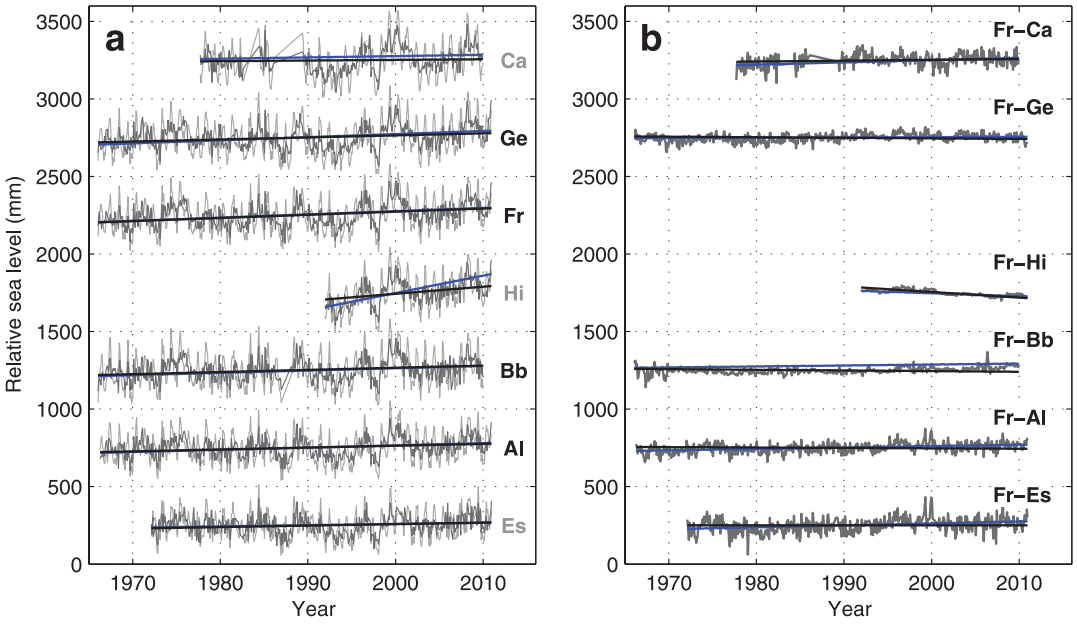

Figure 2. Example sea level time series from southwestern Australia used in the 1966–2011 rate adjustment ordered from northwest to southeast around the coast; see Fig. 4 for tide gauge names and locations. (a) Undifferenced time series: light grey lines include the seasonal cycle, and an average cycle is removed from the data plotted in dark grey. Blue lines are the linear models estimated with CATS, and the black lines show the rate for each site as determined in the least-squares adjustment. Full duration sites are labelled in black, and grey labels indicate shorter duration sites that enter the adjustment only as differential rates with other tide gauges. (b) Differenced time series of each site with respect to Fremantle, with observed and adjusted model rates. Note the removal of much of the energy in the time series compared to Fig. 2(a), particularly for nearby tide gauge pairs.

and offset in addition to annual and semi-annual periodic components (Fig. 2). The CATS software simultaneously solves for the magnitude of white noise as well as the magnitude and character of time-correlated noise in each time series using a MLE approach. We employ a default noise model of white + power-law noise (wh+pl), with the spectral index of the power-law noise (κ), solved as a free parameter, in addition to the magnitudes of white and power-law noise. We also employ an alternative noise model of white + first-order Gauss–Markov noise (wh+gm). In this model, the spectral index is fixed to -2, and there is a parameter for the low-frequency crossover to frequency-independent (white) noise (f_c in eq. 2). The scaling of noise magnitudes employed in the CATS package ensures that power spectra of both noise models cross over at the same frequency given equal noise amplitudes and sampling frequencies (Williams 2003).

Although the wh+pl and wh+gm models have the same number of parameters, MLE fitting commonly identifies wh+gm noise as being more likely, even in cases of the underlying noise being produced by a power-law process (Langbein 2004; Williams & Willis 2006; Santamaría-Gómez *et al.* 2011). The wh+gm model is often estimated as a better fit to data with noise generated by power-law processes as the removal of a trend from raw data reduces the power at the lowest frequencies of the residual time series (S. Williams, personal communication, 2011). Following the previous studies applying this technique to electronic distance measurement, Doppler Orbitography and Radiopositioning Integrated by Satellite (DORIS) and GPS time series, we conducted Monte Carlo tests on 500 synthetic time series with characteristics appropriate to the tide gauge data studied here. The synthetic time series were generated using a power-law noise model with parameters defining the time-series length, periodic signals, noise amplitude and spectral index all representative of those estimated from the 1966–2011 Fremantle record. We use the estimated parameters from Fremantle as its wh+pl noise estimates are representative of all the sites with full records in the 1966–2011 period, and its long duration yields a consistent model for simulating time series of all time spans we consider. We analysed each synthetic time series with CATS using both wh+pl and wh+gm noise models to determine an appropriate log maximum likelihood difference (δML) threshold to reject our null hypothesis of wh+pl noise and accept the wh+gm model. Similar to the results from synthetic time-series representative of continuous GPS (Santamaría-Gómez *et al.* 2011), the 95th percentile corresponds to a δML of 4.1. For time series that exceed this δML, we use the parameter estimates from the wh+gm noise model. Using the same simulated parameters, but changing the spectral index from -1.4 to -0.6 slightly reduces the 95th percentile δML to 3.5, and does not change the outcome of our analysis. The same analysis applied to records of the length and noise character of the 1900–2011 Fremantle record yielded a δML of 1.8 at the 95 per cent level, and we apply this criterion only to records of over a century in length. We have also investigated a white + generalized Gauss–Markov (wh+gg) noise model, in which the spectral index of the noise is estimated as an additional parameter, as well as the magnitude of the Gauss–Markov noise and crossover frequency. In many cases, the wh+gg results included unreasonably high-noise amplitudes, $\kappa < -10$ and very high crossover frequencies. The trade-offs between these three parameters and the fact that the time series that are best fit by a Gauss–Markov process with typical estimated spectral indices $-1 > \kappa > -2$ (when analysed with wh+pl) dictates that the wh+gm model with the value of κ fixed to -2 achieves a similar level of fit with one fewer degree of freedom compared to the wh+gg model. Based on these observations, we consider the white + first-order Gauss–Markov model (wh+gm) to be optimal for time series that are not well-described by power-law noise at low frequencies.

3.1.3 Least-squares adjustment

Estimated linear rates of intersite differences of nearby tide gauge time series generally have much lower uncertainties than those estimated from the time series of individual sites, and are less sensitive to the record duration (Fig. 3). The common-mode ocean signal, which we consider here to be long-period time-correlated noise, is largely removed by the intersite differencing (Fig. 2). As the structure of the noise remaining in the differenced time series is unique to each pair of tide gauges, we obtain many estimates of the relative linear rates between sites with varying levels of estimated uncertainty. While differencing many pairs of tide gauges yields valuable information on the relative rates of sea level change throughout the network, it is clear that not all intersite differences may be treated as independent. A component of the residual noise is shared between differences formed between different pairs of tide gauges, due to the temporal and spatial correlations of what we describe as ocean noise.

Here, we build upon the strategy of Burgette *et al.* (2009) to estimate more precise and accurate rates of relative sea level rise from the network of tide gauges by combining observed rate estimates from the time series of both individual sites and intersite differences in a least-squares adjustment. In addition to incorporating the uncertainties of each rate estimate, we use estimated covariances among all of the observations in the adjustment. Using the observed rates, uncertainties, and associated covariances, we perform an adjustment using generalized least squares (e.g. Montgomery *et al.* 2006) to solve for the adjusted rates of linear sea level rise at all sites for periods beginning in 1993.0, 1966.0 and 1900.0 (Appendix A). As the rates of differences between tide gauges vary less with record length than those estimated from undifferenced time series (Fig. 3), one benefit of this approach is that we are able to obtain robust rate estimates from many shorter duration tide gauge records (compared with the analysis time window, in which at least a significant number of gauges span the full analysis period).

3.2 GPS data and analysis

Our GPS data set includes the 12 continuous GPS sites in Australia with at least 5 yr of data within 100 km of a tide gauge. We use data beginning in 2000.0, excluding noisy, potentially biased data prior to improvements in the global tracking network, in particular the tracking algorithms in receivers that reduced the amount of low-elevation observations in parts of the network (Tregoning *et al.* 2004). The GPS daily position time series are determined with a state-of-the-art analysis of a global network of high-quality GPS stations in the GAMIT/GLOBK analysis suite (Herring *et al.* 2008). The processing method is homogenous through time and includes a number of improvements in modelling atmospheric effects that particularly affect the vertical component of GPS positioning (Tregoning & Watson 2009). Daily positions are determined in the ITRF2008 reference frame (Altamimi *et al.* 2011) using a small set of globally distributed reference sites with minimal hydrological and tectonic deformation (Tregoning *et al.* 2013).

We estimate rates from the vertical components of the GPS time series using the CATS software and a similar strategy to that employed for the sea level time series. We use a variable

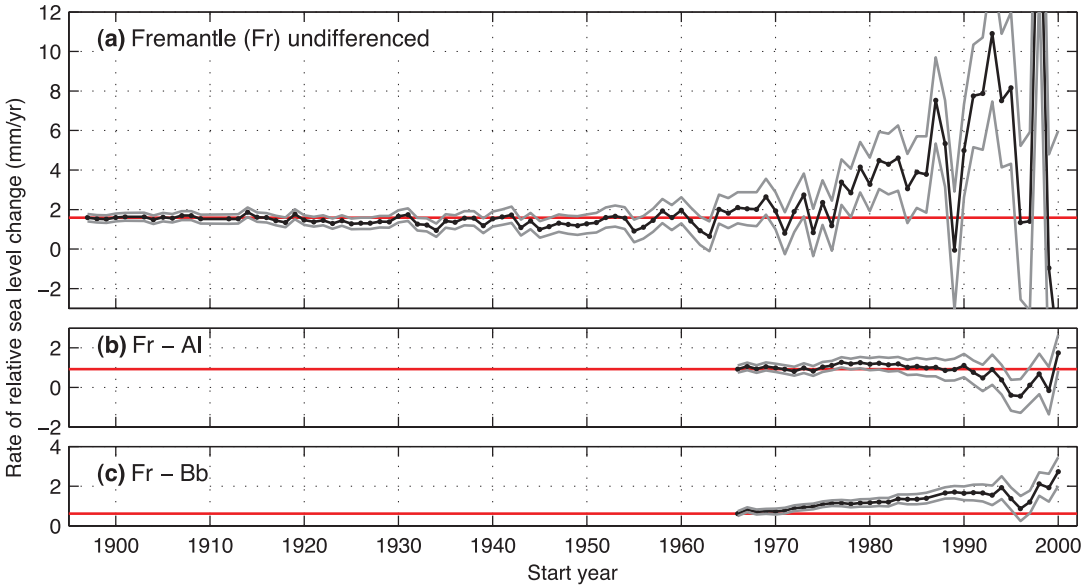

Figure 3. Effect of record length on accuracy of rate estimation. Rates (black line) with one standard error range (grey lines) evaluated with a wh+gm noise model for three representative tide gauge records (see Fig. 2 for time series). Red lines show the rate determined from the full record. Rates estimated from individual site time series (a) are much more sensitive to record length than differences with other regional gauges (b) and (c). The difference of Albany from Fremantle (b), accurately records the relative rate with a record as short as the 1993–2011 altimeter subset. The slightly curved differenced time series involving Bunbury (c) shows a greater discrepancy when shorter subsets are considered; however, for time periods less than 30–40 yr, the estimated rate is less biased than a single undifferenced site.

white + power-law (vw+pl) noise model, simultaneously estimating a seasonal cycle comprising annual and semi-annual harmonics, a linear rate, intercept and step offsets at the times specified in the discontinuity list made available by the International GNSS Service (ftp://igs-rf.ign.fr/pub/discontinuities/soln.snx). We include one additional offset for each of the PERT and HIL1 time series at times of clear discontinuities visible in both the horizontal and vertical components. The variable white noise model uses the formal uncertainty from the GPS processing to appropriately weight each observed daily position estimate. In the absence of a physical explanation for generating power-law noise of a particular index in GPS time series, we estimate the spectral index rather than assuming a single, fixed value for κ, and thus employ the vw+pl noise model. The vw+pl noise model is consistent with the structure of the noise observed in GPS time series (e.g. Santamaría-Gómez *et al*. 2011).

4 RATE OF RELATIVE SEA LEVEL RISE AROUND AUSTRALIA

4.1 Altimeter time period: 1993–2011

The 43 tide gauges in our analysis with data from the period of satellite altimetry (from 1993.0 to 2011.0) provide a relatively dense set of observations of sea level around Australia (Fig. 4; Table 1). The dominant signals in the monthly mean sea level time series are site-specific seasonal cycles, followed by clear ENSO-related interannual energy. We quantify the seasonal cycle by fitting functions with annual and semi-annual periods. The amplitude of the annual variation is dominant at all of the tide gauges, with the median amplitude of the semi-annual signal being 24 per cent of the annual amplitude. Fig. 4 shows the variation in the peak-to-trough range and phase of the seasonal sea level cycle, which varies systematically around the Australian coastline with minimum values in the southeastern quadrant facing the Tasman Sea. The greatest annual changes in sea level occur in tropical north Australia, with maximum ranges of over 1 m in the southern Gulf of Carpenteria, where annual climatic variations interfere constructively (Fig. 4; Forbes & Church 1983). The phase of the yearly cycle shows a similarly smooth pattern of variation. Southern Australia experiences maximum sea levels in the early winter, whereas the northern maxima occur in the austral summer, early in the year.

Over the altimetry period, analysis of the tide gauge time series using CATS and a power-law noise model shows sea level rising around the entire Australian coastline (Fig. 5a), with strong variations that echo the spatial pattern of the seasonal cycles. The mean rate is 8.3 mm yr^{-1}, with a standard deviation (s.d.) of 4.6 mm yr^{-1}. The lowest rates occur in southeastern Australia, and estimated rates exceed 15 mm yr^{-1} at some tide gauges along the northern coast. One must be careful interpreting these values, because over this short time scale, the rates are dominated by the residual ocean noise present in the time series. The uncertainties are, on average, higher by a factor of 6.7 (mean) than what would be estimated if every observed monthly value were considered independent (white noise model). The ratio of uncertainties from coloured versus white noise models has a range of 1.2–22.7, with the high values at the tide gauges with the highest rates. Figs 5c and d show the source of this uncertainty. The noise spectra of the northern Australia tide gauges have spectral indices that approach −2, or random walk noise, limiting our ability to separate the underlying trend of the time series from the superimposed time-correlated noise. Likewise, for a given spectral index, tide gauge records with large amplitudes of power-law noise have greater uncertainties than time series with lower scatter around a linear trend. The δML values do not exceed the 95 per cent confidence limit, and all of the estimates in Figs 5a–d were estimated with the wh+pl noise model.

Applying the generalized least-squares adjustment (Appendix A) to the 1993–2011 data set reduces both the scatter in estimated rates

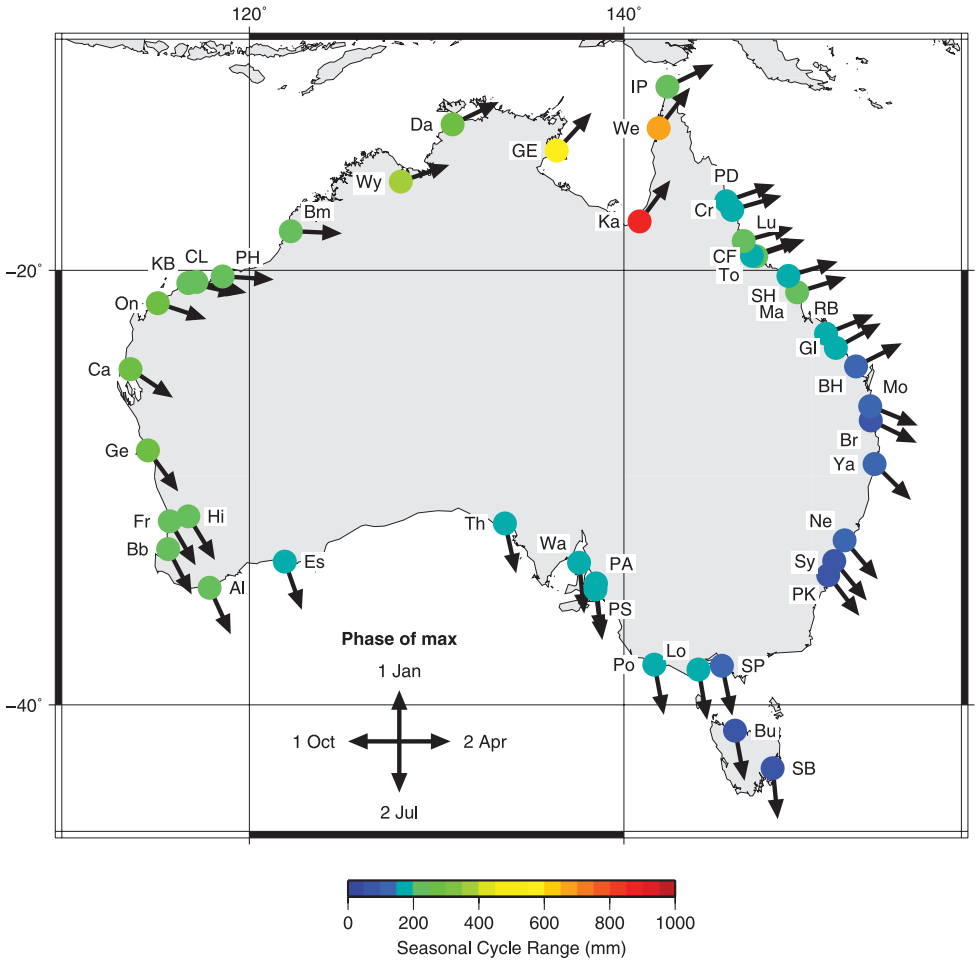

Figure 4. Range (peak-to-trough) and phase of the seasonal sea level cycle from CATS analysis of time series from 1993 to 2011. See Table 1 for names of tide gauges.

as well as greatly reducing the uncertainty of the rates (Figs 5e and f). The intersite differences are less affected by coloured noise, as the mean ratio of uncertainties of wh+pl to white-only noise models is 2.8. The adjustment procedure reduces the influence of common mode noise that changes strongly in character around the perimeter of Australia, while preserving the local and regional variations in the linear rate of change of sea level. The reduced variance of the adjusted data set is purely a consequence of the precise rate differences used in the adjustment. The average rate across the network of tide gauges, accounting for the output variance-covariance matrix of the adjustment, is 4.6 ± 0.8 mm yr^{-1}, (4.8 mm yr^{-1} median, 3.1 mm yr^{-1} s.d.) compared to 8.3 ± 4.6 mm yr^{-1} (mean $\pm$ s.d) for the unadjusted observations. Sea level rise of 3–5 mm yr^{-1} along the eastern and southern coasts is similar to or slightly greater than the global average rate of change for this time period (e.g. Church & White 2011). Considerably more rapid rates of rise occur along the northern and western coasts of Australia, with the highest rates up to 13 mm yr^{-1}. Based on our analysis of longer duration tide gauges in southwestern Australia (Fig. 3), the inputs to the adjustment for the post-1993 period likely contain biases at the >1 mm yr^{-1} level. Particularly, when we note that the southwest coast has a much lower level of annual energy than the north coast (Fig. 4), we treat the high rates estimated for this short time period with caution. A small number of tide gauges have rates that stand out from this broad, smoothly varying pattern of sea level change, such as the Hillarys tide gauge in Perth, Western Australia. In the case of Hillarys, this short spatial scale change in relative sea level change rate corresponds to local vertical land subsidence that has been observed in the Perth area (section 5; Featherstone *et al.* 2012).

4.2 Longer records with wide geographic distribution: 1966–2011

Several tide gauges were installed in the early to middle 1960s around Australia to establish the Australian Height Datum. We use the same end time (2011.0) and choose 1966.0 as the starting year for the second analysis window, as it corresponds to a temporally homogeneous data set of 14 tide gauges that circle Australia with interstation spacing close enough for regional noise to be relatively highly correlated across neighbouring stations. The 45-yr time-series length of this window approaches previous estimates for the minimum data length needed to adequately resolve linear trends in sea level data from individual records (e.g. Douglas 1991).

The variation in observed rates from the individual time series for the 1966–2011 analysis (Figs 6a and b) is lower than the more recent post-1993 window (Figs 5a and b), reflecting a reduced effect of time variable noise on trend estimation. The average rate is 2.1 ± 1.0 mm yr^{-1} (mean $\pm$ s.d.), and a median of 1.8 mm yr^{-1}. The mean uncertainties are lower relative to a white-only noise model than those estimated from the 1993–2011 window, with a mean factor of 3.6. The spatial pattern is broadly similar to that estimated from the

Table 1. Tide gauge names, locations, durations, and adjusted rates and uncertainties from the 1900–2011 adjustment.

Abbrev	Tide gauge name	Lon (°)	Lat (°)	Start	End	Adjusted rate (mm yr^{-1})	Uncertainty (mm yr^{-1})
PD	Port Douglas 2	145.467	−16.483	1987.96	2009.96	2.57	0.81
Cr	Cairns	145.783	−16.917	1966.04	2009.96	1.30	0.44
Lu	Lucinda	146.383	−18.517	1985.45	2010.96	2.80	0.49
CF	Cape Ferguson	147.058	−19.277	1991.79	2010.96	1.92	0.49
To	Townsville I	146.833	−19.250	1959.04	2010.96	0.84	0.37
SH	Shute Harbour 2	148.783	−20.283	1990.20	2010.96	1.04	0.73
Ma	Mackay	149.233	−21.100	1966.04	2010.96	1.56	0.44
RB	Rosslyn Bay	150.790	−23.161	1993.29	2011.79	1.05	0.42
Gl	Gladstone	151.314	−23.854	1978.04	2010.96	1.20	0.60
BH	Bundaberg, Burnett Heads	152.383	−24.767	1980.04	2010.96	0.33	0.44
Mo	Mooloolaba 2	153.133	−26.683	1979.62	2010.96	0.09	0.52
Br	Brisbane (West Inner Bar)	153.167	−27.367	1988.04	2010.96	2.40	0.36
Ya	Yamba	153.362	−29.430	1989.54	2010.45	−0.67	1.03
Ne	Newcastle V	151.789	−32.924	1966.04	2010.96	0.84	0.29
Sy	Sydney	151.226	−33.855	1900.00	2010.96	0.73	0.22
PK	Port Kembla	150.912	−34.474	1991.62	2010.96	1.44	0.35
SB	Spring Bay	147.933	−42.546	1991.45	2010.96	1.63	0.59
Bu	Burnie	145.915	−41.050	1992.71	2010.96	1.10	0.49
SP	Stony Point	145.225	−38.372	1993.04	2010.96	0.19	0.56
Lo	Lorne	143.989	−38.547	1993.12	2010.96	0.21	0.56
Po	Portland	141.613	−38.343	1982.12	2010.96	0.81	0.46
PS	Port Stanvac	138.467	−35.109	1992.54	2010.87	2.21	0.64
PA	Port Adelaide (Inner)	138.511	−34.830	1933.04	2008.96	1.83	0.37
Wa	Wallaroo II	137.615	−33.926	1986.29	2010.96	−0.31	0.99
Th	Thevenard	133.641	−32.149	1965.45	2010.96	0.82	0.36
Es	Esperance	121.895	−33.871	1972.12	2010.96	0.74	0.34
Al	Albany	117.893	−35.034	1966.29	2010.96	1.06	0.30
Bb	Bunbury	115.660	−33.323	1966.04	2009.96	1.11	0.26
Fr	Fremantle	115.748	−32.066	1900.00	2010.96	1.78	0.24
Hi	Hillarys	115.739	−31.826	1991.96	2010.96	4.34	0.43
Ge	Geraldton	114.602	−28.776	1966.04	2010.96	1.17	0.28
Ca	Carnarvon	113.651	−24.899	1977.71	2009.96	0.41	0.50
On	Onslow	115.132	−21.650	1985.54	2010.96	0.96	0.55
KB	King Bay	116.749	−20.624	1982.79	2008.96	0.96	0.55
CL	Cape Lambert	117.186	−20.588	1983.71	2010.96	0.89	0.57
PH	Port Hedland	118.574	−20.318	1966.04	2010.96	2.09	0.51
Bm	Broome	122.219	−18.001	1991.96	2010.96	2.54	0.68
Wy	Wyndham	128.101	−15.453	1984.62	2009.96	4.20	0.82
Da	Darwin	130.846	−12.472	1959.12	2010.96	2.12	0.65
GE	Groote Eylandt	136.416	−13.860	1993.79	2010.96	4.07	1.03
Ka	Karumba	140.833	−17.500	1985.04	2010.96	4.48	1.24
We	Weipa	141.867	−12.667	1966.04	2010.96	3.35	1.02
IP	Ince Point	142.310	−10.508	1998.62	2009.96	6.23	1.99

shorter time spans, with the highest rates in the north and west, and lower rates to the southeast. All of the time series from tide gauges in the western two-thirds of Australia are better fit by a wh+gm noise model than wh+pl at the 95 per cent confidence level, perhaps suggesting a boundary between different noise processes generated in the Indian and Pacific Oceans (Figs 6c and d). Despite this boundary between noise models, both the estimated uncertainties on the rates and time-correlated noise amplitudes follow a fairly smooth pattern of variation. The spectral indices of the sites fit by the wh+pl model (Fig. 6c) are generally closer to white noise than what is inferred from the shorter 18 yr period (Fig. 5c).

To refine and densify the estimates of sea level rise over the 1966–2011 period, we perform a second least-squares adjustment, with inputs comprising the observed rates of the 14 sites with complete time series (Figs 6a and b) and rates of differences involving all 43 tide gauges of varying record length (in most cases longer than those input into the previous adjustment). Although the approximation that the rates of intersite differences are independent of the time-series length is not perfect (Fig. 3), this adjustment provides uncertain estimates of the rates that would have been measured if all the tide gauges were present over this full interval. The mean rate estimated from the full network considering the output uncertainty and covariance is 1.7 ± 0.6 mm yr^{-1}, with a standard deviation of 1.5 mm yr^{-1}, and a 1.6 mm yr^{-1} median. Using the rates derived from longer time series lowers both the magnitude and variability of estimated sea level rise around Australia in comparison to the 1993–2011 data set (Figs 6e and f). The estimated rates of the 14 full duration sites do not change greatly in the adjustment, although the average rates and variation among sites are reduced: 1.9 ± 0.8 mm yr^{-1} (mean ± s.d.), and the median is 1.5 mm yr^{-1}. These results reflect the general correlation we observe in this data set between lower estimated uncertainties and lower rates of sea level rise (Figs 6a and b), and the generally lower magnitudes of sea level change estimated between sites using differenced time series in contrast with comparisons made with rates estimated from single-site time series.

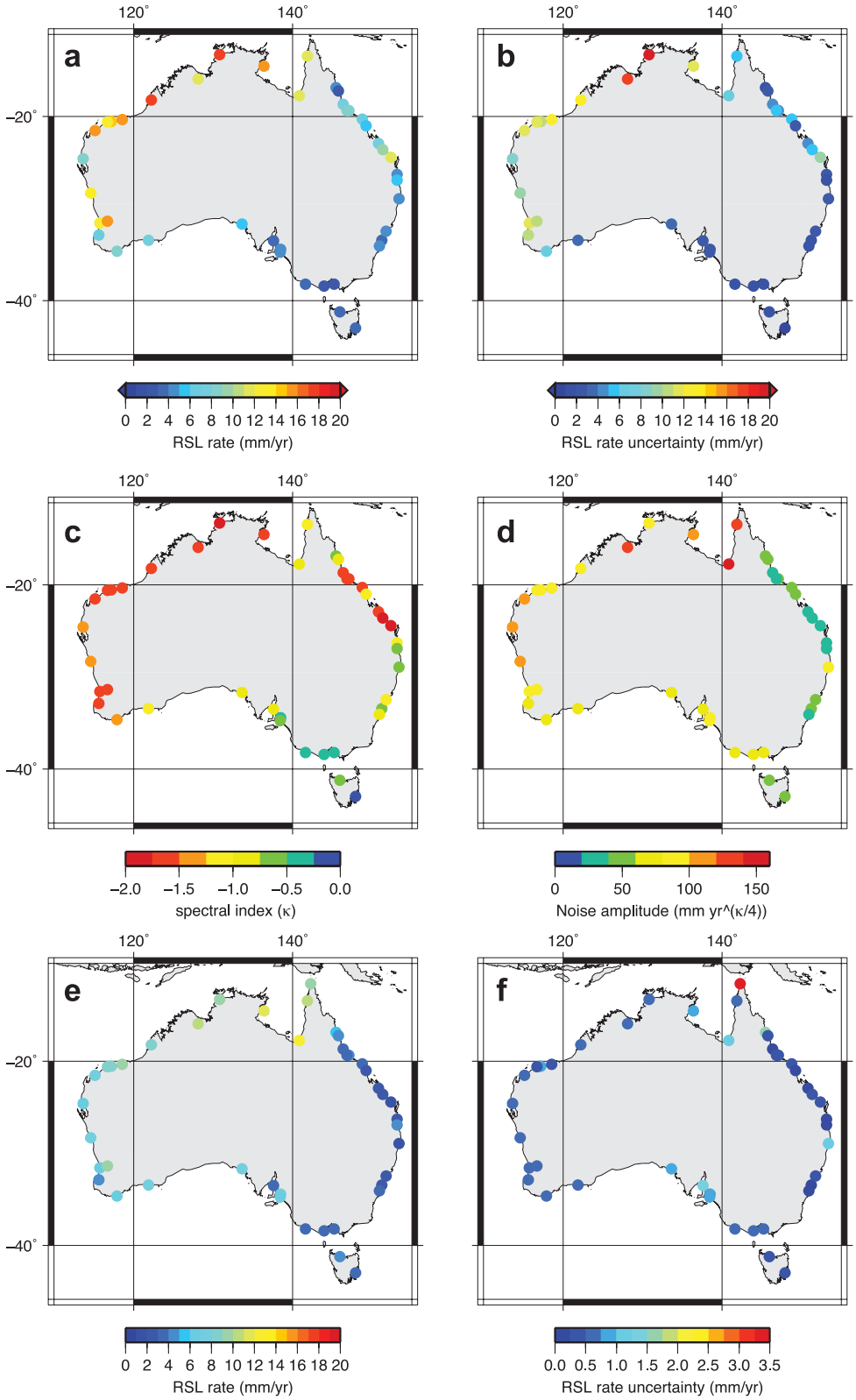

Figure 5. Results of 1993–2011 analysis. Rate of relative sea level (a), uncertainty (b), spectral index (c) and power-law noise amplitude (d) of time series estimated with CATS analysis. The least-squares adjustment lowers intersite variation of rates (e) and improves estimated rate uncertainties (f).

The less pronounced longitudinal and latitudinal gradients in the rate of sea level rise around the continent allow greater resolution of finer spatial scale variations in the adjusted rates (Fig. 6e). Some of the short-wavelength variations in the rate of relative sea level change are clearly related to local processes, such as the Perth (Hillarys and Fremantle) and Gulf St Vincent (Port Adelaide, Wallaroo and Port Stanvac) areas, and possibly others. However, some of the shorter spatial scale variation is related to spurious effects

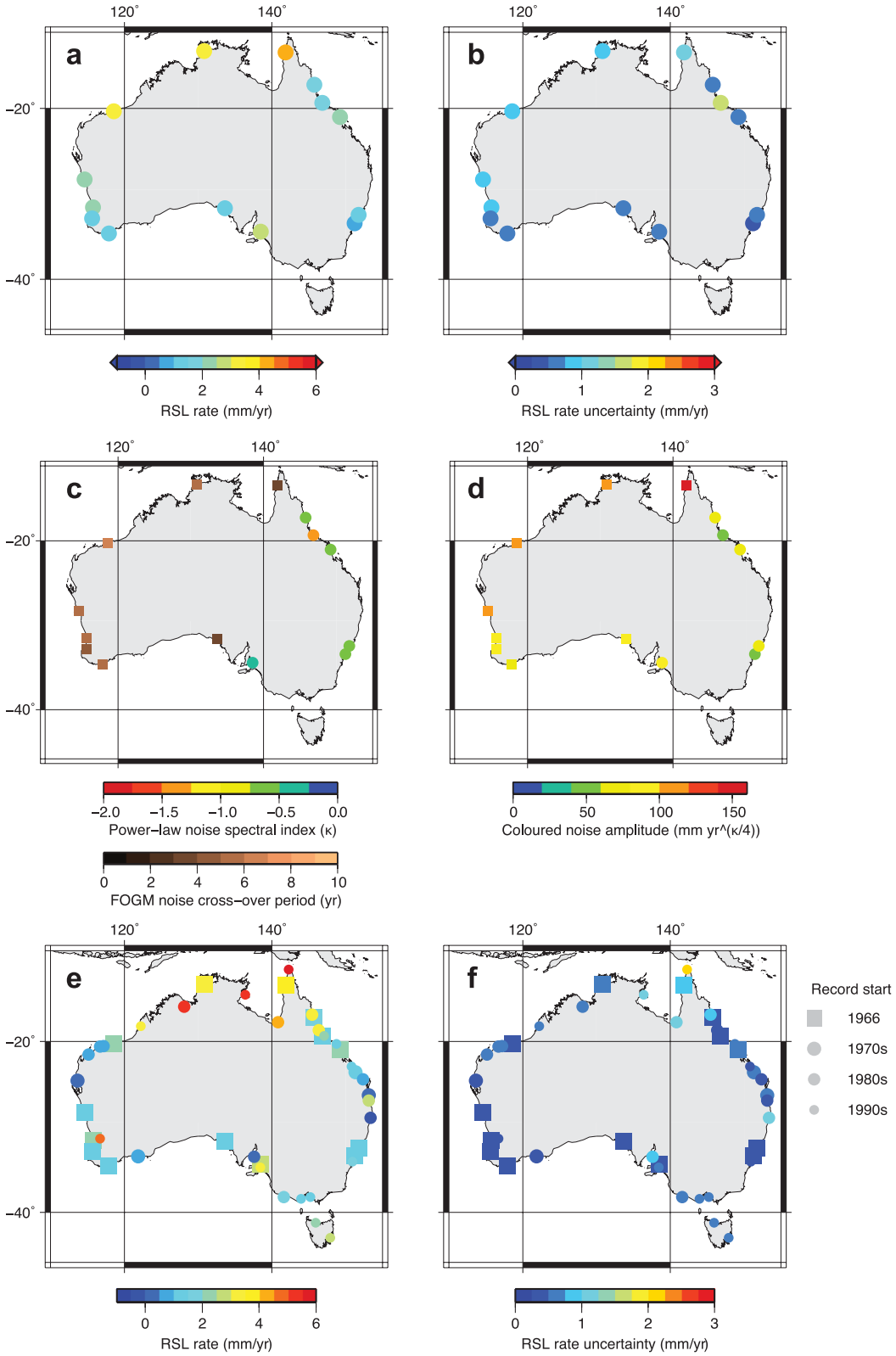

Figure 6. Results of 1966–2011 analysis. Rate of relative sea level (a), uncertainty (b), spectral index/crossover period (c) and coloured noise amplitude (d) of time series estimated with CATS analysis. Square symbols indicate that first-order Gauss–Markov is the preferred noise model at the 95 per cent confidence level, and circles indicate that power-law noise better fits the time series. Rates (e) and uncertainties (f) from the least-squares adjustment that estimates rates at all sites over this period. Large square symbols indicate tide gauges with full duration records, and circles correspond to shorter duration tide gauges that enter the adjustment only with differenced rates. Note change in colour scales for rate estimates from Fig. 5.

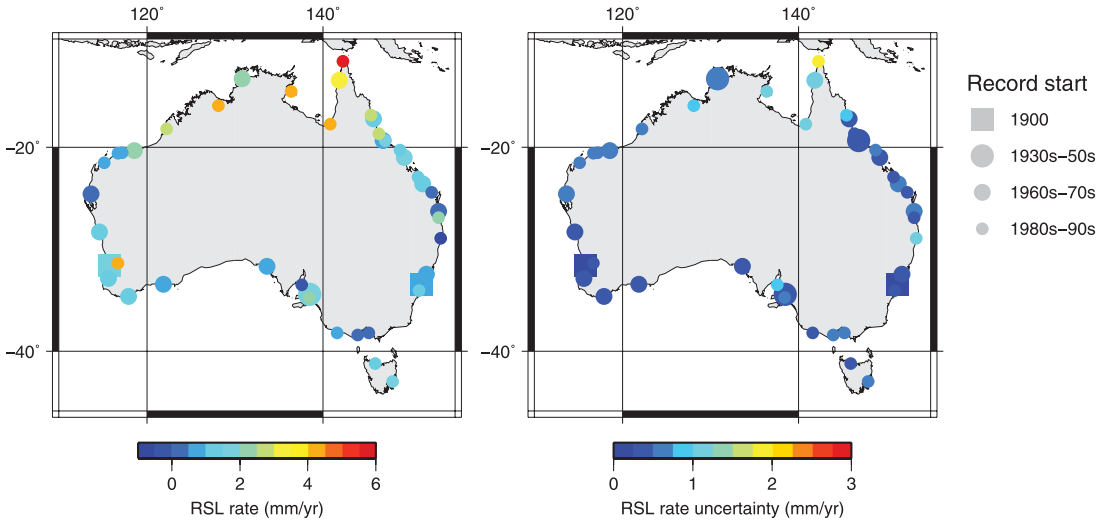

Figure 7. Results of the 1900–2011 adjustment. The only input rates of undifferenced time series are from Sydney and Fremantle (square symbols). Numerical values are listed in Table 1.

of noise in the differenced time series being different in character from the full 1966–2011 set (e.g. Fig. 3). An example of this comes from the three sites on the central east coast (Yamba, Brisbane and Mooloolaba) that show scattered rates, but correspond with relatively large estimated uncertainties.

4.3 Longest records: 1900–2011

The longest records of consistent length begin in the late 1800s at Fremantle and Sydney. We determine rates for subsets that begin at 1900.0 for comparison with other sea level estimates with this start time. Exclusion of the first 3 yr of Fremantle's record negligibly affects the calculated rate of sea level rise (Fig. 3). As for the 1966–2011 time window, Fremantle is best fit by wh+gm and Sydney is better matched by wh+pl (Fig. 1). The full time series of the other 41 sites are used in forming intersite differences whose rates and uncertainties enter the adjustment by generalized least squares (Fig. 7). Overall, the spatial pattern of sea level rise is generally similar to the results of the 1966–2011 adjustment (Fig. 6e). The same sites generally exhibit short spatial wavelength variations in the rate of sea level change. In comparison to results from the shorter intervals, the rates are shifted to lower values, reflecting the lower rates of sea level rise (lower by 0.5 and 0.2 mm yr^{-1} for Fremantle and Sydney, respectively) estimated over this longer period. Propagating uncertainties from the adjustment, the network average rate is 1.4 ± 0.6 mm yr^{-1}. The standard deviation of the 43 sites is 1.4 mm yr^{-1}, and the median value is 1.2 mm yr^{-1}. The faster rate for the more recent analysis period is consistent with an acceleration sea level rise through the twentieth century (e.g. Church & White 2011), but may also be an indication that the ∼45 yr time period for the 1966–2011 data set is insufficient to obtain a robust linear rate that is insensitive to the effects of interannual and decadal climatic variations that have been observed in sea level time series (e.g. Feng *et al.* 2004; Chambers *et al.* 2012). However, we note that the phase of a ∼64 yr period oscillation in sea level (Chambers *et al.* 2012) would be basically the same at the start years of the intervals in 1900 and 1966. If this fluctuation describes the dominant multi-decadal variation in sea level, it may not have a strong effect on trends calculated over the intervals we have analysed.

5 RATES OF VERTICAL LAND MOTION AND GEOCENTRIC SEA LEVEL CHANGE

Our observed vertical land motion rates from the GPS time series show that the vertical deformation of the coast of continental Australia is occurring at generally low rates, consistent with the distance from active plate boundary zones (Fig. 8a). The majority of the GPS sites do not exhibit rates that are significantly different from zero at the one standard error level (Figs 8a and b). Only three of the sites show significant vertical displacement rates at the 2−σ level, with HIL1 (−3.1 ± 0.7 mm yr^{-1}) and PERT (−2.1 ± 0.7 mm yr^{-1}) showing significant subsidence, consistent with the ITRF2008 solution (Altamimi *et al.* 2011). The uplift at YAR2 (0.9 ± 0.4 mm yr^{-1}) appears higher than the ITRF2008 solution (0.1 ± 0.4 mm yr^{-1}), but in closer agreement with solutions from other analysis centres (e.g. JPL: 0.5 ± 0.4 mm yr^{-1}). The source of these differences and the suggestion of uplift remain unexplained.

Similar to the tide gauge data, the GPS time series with the greatest time correlation and largest magnitude noise occur in the northern portion of Australia (Figs 8c and d). Larger noise magnitudes at lower latitude GPS sites have been observed in global analysis of noise in GPS time series (Williams *et al.* 2004). This is most evident at DARW, where we estimate subsidence at a rate of −1.6 ± 1.4 mm yr^{-1}, and large magnitudes of hydrological deformation are observed (Tregoning *et al.* 2009). Given the difference in sampling periods for the two data sets and the scaling scheme used in CATS (Williams 2008), the noise amplitudes for the daily GPS data are higher by a factor of 2.3 than a data set sampled at a monthly period with the same level of spectral power, when flicker noise is considered. Hence, the level of noise in the GPS time series is an order of magnitude lower than what we observe in the sea level time series (Figs 6d and 8d), and consistent with achieving equivalent uncertainties on rates when using only several years of GPS data in contrast to the decades needed for tide gauge data (Figs 6b and 8b).

To assess the influence of vertical land motion on tide-gauge-based inferences of absolute sea level rise around Australia, we compare the vertical land motion rates determined from the GPS analysis to the relative sea level rates determined in the 1900–2011 adjustment (Fig. 9). The data generally follow an inverse

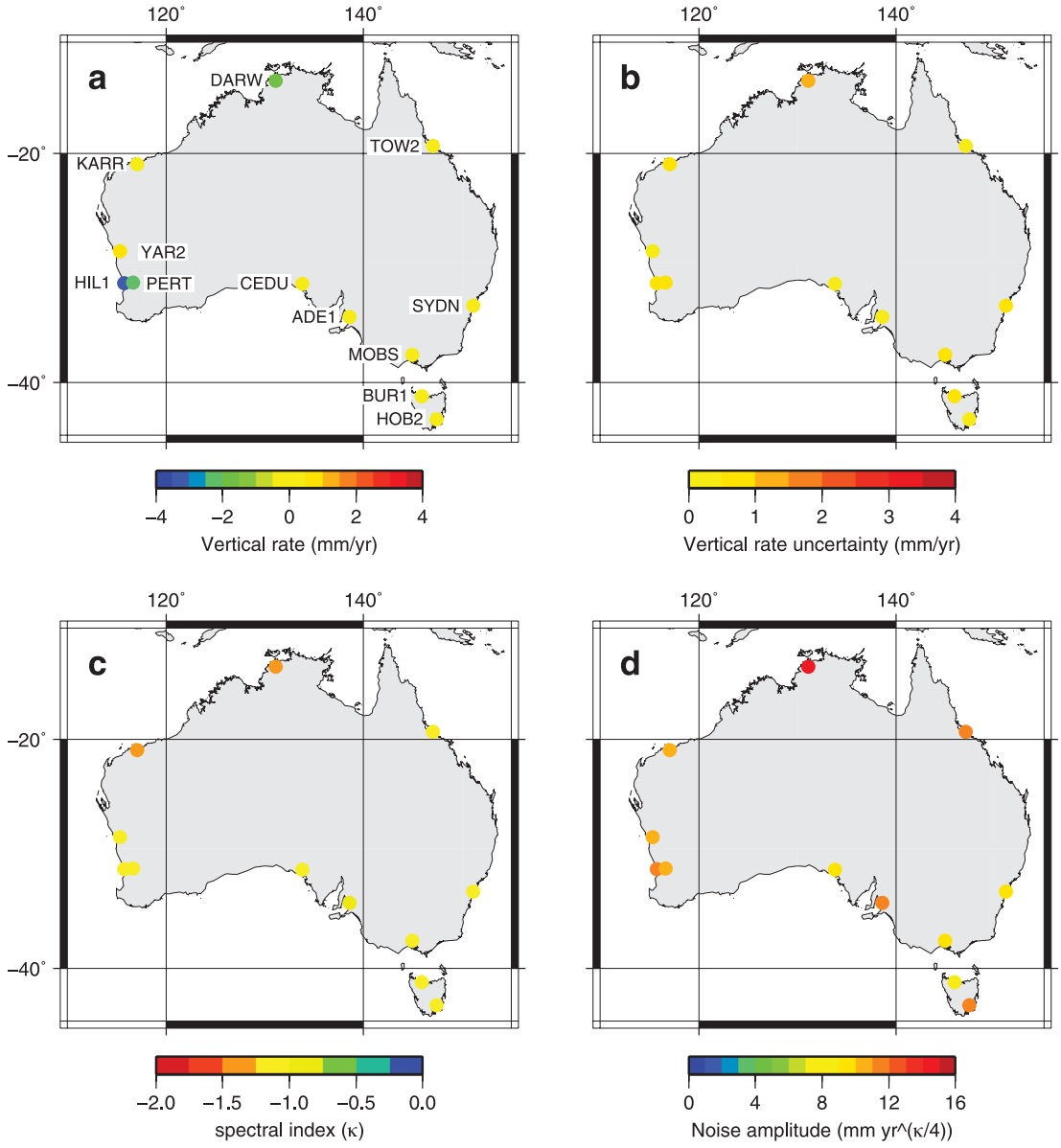

Figure 8. Uplift rates (a) for continuous GPS sites around the coast of Australia, associated uncertainties (b), spectral indices (c) and power-law noise amplitudes (d) from CATS fitting. The symbol for PERT is offset for clarity.

relationship between crustal uplift rate and rate of relative sea level rise, although the scatter suggests that crustal deformation is not the primary control on the pattern of relative sea level change. The lower range of vertical land motion rates results in a less well-defined relationship than those observed in areas of active tectonism and postglacial isostatic adjustment (e.g. Milne *et al.* 2001; Mazzotti *et al.* 2008; Woodworth *et al.* 2009a). The reference line in Fig. 9 represents a hypothesis that the mean rate of sea level rise from our adjustment (1.4 mm yr^{-1}) represents an accurate estimate of the rate of geocentric sea level rise, and that this rate of sea level rise is constant around the coastline. Nearly all of the data fall within two standard errors of this line for both the sea level and GPS data. Some of the departures from this hypothesis result from the regional deviations from a continent-wide, constant rate of sea level change. Notably, most sites in the comparison are from southern Australia (Fig. 8) where estimated rates of sea level are lower than the mean. Another component of the scatter is due to the adjustment procedure not removing all of the biases in the linear rates caused by interannual and decadal sea level variations at the tide gauges, as discussed in Section 4.

Another complication in making such comparisons with the current data set is the separation between tide gauges and GPS of several kilometres to several 10 s of kilometres (Fig. 9). In the Adelaide and Perth areas, where subsidence has been identified in previous studies (Belperio 1993; Ananga *et al.* 1995; Featherstone *et al.* 2012), we find significant differences (up to 2.5 mm yr^{-1} difference in relative sea level rates over distances of <30 km). This short-wavelength variation in vertical rate caused the discrepancy in the Perth area in a global study that compared the GPS rate at the PERT site to the Fremantle tide gauge (Bouin & Woppelmann 2010). The tide gauges in the area around Adelaide show a 2.6 mm yr^{-1} difference in relative sea level rise over 150 km distance between Port Stanvac and Wallaroo. Considering the short spatial scale of the variation in subsidence rates inferred in the area (Belperio 1993; Ananga *et al.* 1995), and the 17 km separation between the Port Adelaide tide gauge and the ADE1 GPS site, it is difficult to quantify the rate

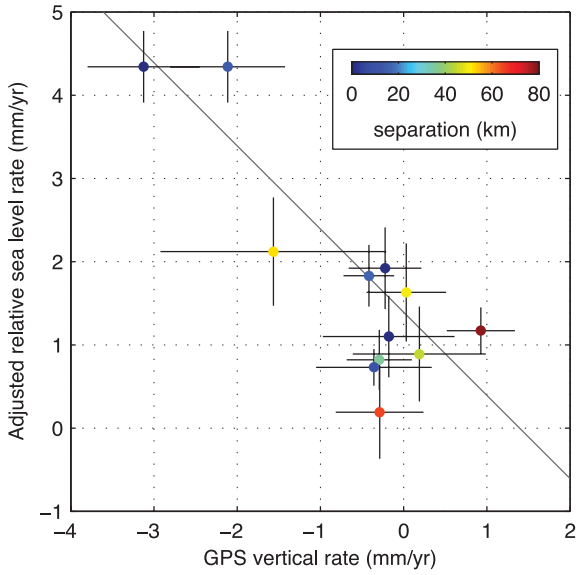

Figure 9. Comparison between relative sea level rates from the 1900–2011 adjustment and the vertical rates derived from the GPS time series. Error bars are $1-\sigma$ for both data sets. The tide gauge–GPS pairs are selected as the nearest tide gauge to each of the GPS sites, and are all unique except for the Hillarys tide gauge and both the HIL1 and PERT GPS stations. Points are coloured by the distance separating the GPS and tide gauge sensors for each pair. The grey reference line has a slope of -1 and an offset of 1.4 mm yr^{-1} (the mean rate of the full sea level data set).

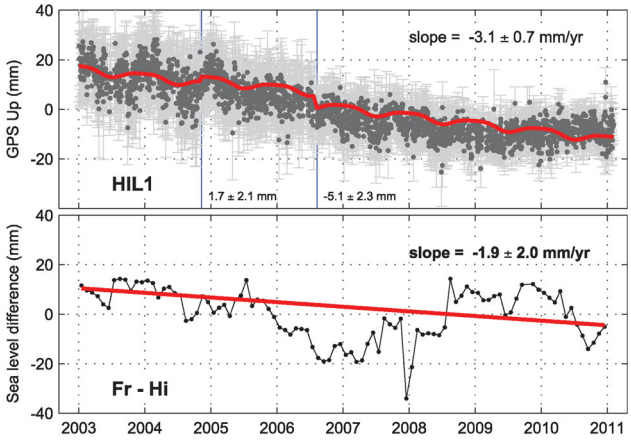

Figure 10. The HIL1 GPS time series and Fremantle–Hillarys tide gauge differenced sea level time series over their common interval. Blue lines in the top panel show times at which step offsets are estimated. The red lines and reported slopes are the CATS wh+pl model fits to the data. Note the relatively poor fit of the linear model to the GPS and sea level data, with a suggestion of a reduction in the rate of subsidence in the GPS record at 2008.5.

of geocentric sea level rise in this region of South Australia with confidence.

The most rapid rate of relative sea level rise in our comparison data set occurs at the Hillarys tide gauge, with the co-located HIL1 GPS receiver that records the maximum subsidence rate of -3.1 ± 0.7 mm yr^{-1} (Fig. 9). More careful analysis of the tide gauge and GPS time series gives insight into the potential effects of temporal variations in rates of crustal deformation (Fig. 10). The Fremantle and Hillarys tide gauges are among the most closely spaced of the Australian network (27 km), and there is relatively low noise in the differenced time series from the two tide gauges (Fig. 2b). The overall variability of the sea level difference and GPS time series are similar, with standard deviations of 10.3 and 10.4 mm (8.9 mm with offsets and seasonal cycle removed), respectively. Although there is no GPS receiver co-located with the Fremantle tide gauge, its lower rate of relative sea level rise (1.6 ± 0.2 mm yr^{-1} over 1900–2011) is consistent with this site being approximately stable. Assuming that the Fremantle tide gauge is stable, the difference of the Hillarys time series from Fremantle should reflect the vertical rate of Hillarys, directly comparable to the HIL1 GPS time series (Fig. 10).

Vertical deformation at HIL1 does not appear to have occurred at a constant rate, with an apparent slowing of subsidence around 2008.5 (Fig. 10, see also Featherstone *et al.* 2012). Although over such short time spans the sea level difference rate is imprecise, there is a suggestion that the differential sea level record shows a similar slowing in the rate of subsidence at Hillarys. The full Fremantle–Hillarys time series shown in Fig. 2 shows similar character of highly correlated values over short time scales, but with longer wavelength apparent changes in rates. Subsidence in the Perth area has been linked to groundwater extraction (Featherstone *et al.* 2012). The Perth area is subject to rapid rates of groundwater depletion, and the rates of lowering of the water table are not constant through time (Bekesi *et al.* 2009). However, quantitatively explaining the temporal variation in subsidence is beyond the scope of this study. If rates of subsidence have changed through time in this area, as the GPS data suggest, comparisons such as Fig. 9 should be made with similar temporal records of co-located GPS and tide gauges. This location in Western Australia will provide a good example to answer such questions as both data sets grow in length and increase in precision.

6 DISCUSSION

6.1 Relative and absolute sea level change around Australia

In making the assumption that the underlying signal of sea level rise is perfectly linear, we treat all other residual energy as 'noise' and recognize that much of this is, in fact, a different signal that is highly spatially and temporally correlated and related to shorter period (interannual to decadal) climate variability. Our adjustment strategy provides a mechanism to attenuate this variability component, as much of the variability is removed when forming local intersite differences in sea level. The output from our adjustment enables us to precisely image the pattern of spatial variation in the linear rate of sea level rise around the Australian coastline.

Our analysis of the Australian tide gauge network shows generally smooth spatial variations in the underlying linear rate of sea level rise (relative to the land), with exceptions at locations with known ground subsidence issues. The GPS-measured rates of vertical crustal deformation are consistent with the majority of the geodetic sites not experiencing statistically significant rates of vertical movement. Taken together, these observations suggest that the rates of relative sea level change from the higher quality tide gauges are not statistically significantly different from geocentric sea level rise around the Australian coastline within the current levels of uncertainty in both the GPS and tide gauge observing systems. The mean rates of sea level rise around Australia are similar to, or slightly higher than those inferred globally for similar time

periods (Church *et al.* 2004; Church & White 2011). The $\sim 2 \pm 1\,\mathrm{mm\,yr^{-1}}$ higher rates of sea level rise we observe in northern Australia relative to the southern shoreline are greater than, and in the opposite sense of, the $0.4\,\mathrm{mm\,yr^{-1}}$ signal predicted for ongoing glacial isostatic adjustment (GIA) across the region following the most recent Pleistocene glaciation and associated change in water loading (e.g. Fleming *et al.* 2012). The scatter remaining in the adjusted sea level rates, and the likely influence of climatic variability on the rates we estimate here suggest that a dense set of high-quality century-scale tide gauge records would be required to observe effects of GIA at the magnitudes predicted for Australia.

When estimating a sea level rate from a single tide gauge time series over a nominated time period, the rate will contain the effects of interannual to decadal ocean variability, and thus be different from the desired underlying secular rate of sea level rise, which we assume is constant. If the time correlation of the 'noise' is taken into consideration, the uncertainty about the estimated rate will reflect the contribution from ocean/climate variability. For sites in northwestern Australia, over the shorter altimetry period, such an estimation using CATS and a realistic noise model yields rates in excess of $15\,\mathrm{mm\,yr^{-1}}$, with comparably large uncertainties (Figs 5a and b). Given the large uncertainties and the context provided by analysing longer time periods, such estimates should not be taken seriously as representing long-term sea level rise. Over the same period, our adjustment technique minimizes the contribution of the variability in an attempt to extract the underlying linear signal. On first inspection, the uncertainties from our adjustment process appear overly optimistic: they describe the statistical variation in the underlying adjusted linear trend and should not be interpreted as including the full contribution from ocean variability.

Simple unweighted least-squares estimation of rates from individual site time series indicates that the differences in relative sea level rates between the 1993–2011 and 1966–2011 data sets are highly significant for many tide gauges. However, the CATS fitting procedure accurately identifies the uncertainty in the estimated sea level rates due to the presence of time-correlated noise, and yields consistent rates and uncertainties for different subsets of the same time series. This emphasizes that longer time series are needed to conclusively identify the geographic variation of the long-term trend of sea level rise around Australia at levels approaching what we can achieve at Fremantle and Sydney currently, and that the time-correlated noise must be taken into consideration when estimating the linear trends.

The long time series necessary to minimize the biases of time-correlated noise for estimating linear trends are problematic should the underlying signal of long-term change significantly deviate from linear change. Global compilations (e.g. Woodworth *et al.* 2009b) show acceleration in sea level rise over the span of tide gauge data. Given the level of noise we observe in the individual time series we studied here, it seems unlikely that a simple linear model could be rejected with a high level of confidence in favour of a quadratic model for any of the individual Australian tide gauge time series. However, acceleration in the time series will not be fit by the linear model we employ and will add to the low-frequency power in the residual time series, biasing estimates of time-correlated noise and uncertainty to higher values than if we truly knew the form of the underlying sea level change signal. Likewise, potential time variations in crustal deformation rates, as is suggested for the Perth area (Fig. 10), will bias rates and associated uncertainties for both GPS and sea level time series when analysed assuming a linear model.

6.2 Implications for future higher precision sea level rates

The large rate uncertainties estimated for individual sites using CATS for the sea level data set are consistent with the inference from previous tide gauge studies (e.g. Douglas 1991) that time series of several decades in length are necessary to precisely and accurately resolve an underlying linear rate in the presence of noise commonly found in individual tide gauge records (Fig. 3). This point is emphasized by comparison to an earlier study of the spatial variation of relative sea level change around Australia, which found relative sea level fall in northern Australia, and more rapid sea level rise to the south (Aubrey & Emery 1986). With a growth in length of the observational data set of over a decade, we find the opposite geographic pattern of relative sea level change (Fig. 7). Given that the early portion of our records is the same as was analysed in this previous study, we infer that decadal fluctuations bias trend estimates made on short time intervals of two decades (e.g. Zhang & Church 2012), and possibly the current 45 yr records at many tide gauges. These observations motivate better understanding of the relationship between time-series length and rate uncertainty in the presence of significant interannual oceanic variability, which is treated in our study as time-correlated noise.

Our time-series analysis yields estimates of the noise types and associated parameters for the Australian tide gauge records (Figs 5 and 6). The longer duration records of the 1966–2011 data set appear to characterize the noise in the time series more accurately than the 1993–2011 data. Fig. 11 shows predicted standard errors of linear rates given the noise levels and other spectral information estimated from the tide gauge time series using CATS. We use representative noise parameters of the multiple sites in the groups best fit by wh+pl and wh+gm noise, and expressions derived from the noise covariance matrices appropriate for the coloured noise models (Williams 2003, S. Williams, personal communication, 2012). The mean values for the two coloured noise models follow similar trajectories, with a crossover in uncertainty levels at approximately 75 yr, with more precise rates from power-law noise for shorter records, and

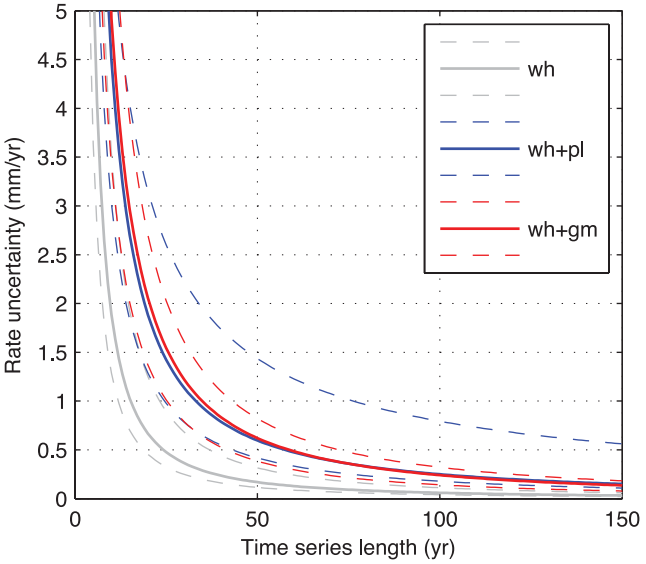

Figure 11. Predicted time evolution of uncertainties of relative sea level rates based on noise parameters estimated from Australian tide gauge records. The solid line for each noise type is generated with the median noise parameters for that noise type in the 1966–2011 data set (Figs 6c and d), and the dashed lines below and above use the minimum and maximum uncertainties estimated from these data, respectively.

more precise rates from first-order Gauss–Markov noise for longer records. There is broad overlap between the bounding curves for the two coloured noise models and little overlap with predictions made assuming a white noise-only model. The highest uncertainty wh+pl noise model parameters show a much weaker decay in the rate uncertainty with time-series length than what is inferred for the other noise models. Considering the median models, we will be able to resolve variations in sea level change rate from undifferenced time series at most of the sites in the 1966-onward tide gauges at the 0.5 mm yr^{-1} level with an additional 15 yr of observation. Yet, another ∼40 yr will be required to double the precision to the 0.25 mm yr^{-1} level, if the estimated noise parameters accurately characterize the noise process affecting individual Australian tide gauges. Such levels of precision are necessary to quantify the spatial variation of relative sea level rise associated with the isostatic response to past and future glacial ice loss, a signal with a magnitude of ∼ 0.5 mm yr^{-1} or less over the spatial scale of Australia (Fleming *et al.* 2012). This provides further motivation for maintaining a dense network of long-term consistent tide gauge sensors.

6.3 Tide gauge stability

The existing network of GPS receivers near tide gauges in Australia is helpful in assessing the vertical motion of the broader setting of the nearest tide gauges, but only the co-located tide gauges and GPS antennas at Hillarys and Burnie currently allow direct monitoring of the geocentric stability of the tide gauges. The situation is improving with GPS receivers installed in the last 4 yr at or near many more tide gauges as part of the AuScope initiative (Coleman *et al.* 2008). GPS receivers do not need to be precisely co-located with tide gauges to monitor tide gauge stability, and in some cases benefit by being positioned away from the immediate tide gauge vicinity, as long as relatively regular ties are made between the tide gauge sensor by levelling and/or additional GPS observations (Bevis *et al.* 2002).

Another key way to monitor tide gauge stability is through maintaining a spatially dense network of tide gauges. The high correlation of noise in the time series means that relatively small offsets or changes in rates can be identified from the differenced time series, and problematic tide gauges may be identified if anomalies are present in differences with at least two neighbours. This process works at a much higher level of precision for the Australian network since the 1990s. Careful re-analysis of the levelling records of several tide gauges in the PSMSL RLR data set from the west coast of the United States showed that portions of the time series were biased by up to 1.6 mm yr^{-1} in both positive and negative senses due to local benchmark instabilities (Burgette *et al.* 2009). Even these significant levels of instability are difficult to definitively detect in differenced time series and motivate retrospective analyses of datum stability where the data are available.

The region around the long-running Fort Denison tide gauge in Sydney Harbour is a strong candidate for better geodetic monitoring, given its importance for constraining sea level over more than a century. Although likely not significant given the current record length, the ABSLM tide gauge at Port Kembla, which is 75 km south of the Fort Denison tide gauge, shows a more rapid rate of sea level rise by ∼0.6 mm yr^{-1} compared to Fort Denison. The small island position of Fort Denison precludes assessing relative stability of the tide gauge beyond its local setting using terrestrial surveying methods, but a GPS site, FTDN, was installed at Fort Denison in 2012. Likewise, it is difficult to assess the stability of the Port Kembla tide gauge on a regional basis with the current tidal benchmark levelling. The discrepancy in rate between Sydney and the long-running tide gauges at Newcastle 116 km to the north led Douglas (1991) to exclude both of these sites from a global compilation. The difference in rate at Newcastle has since been attributed to mining-related subsidence (Watson 2011), and we do not use data from Newcastle area tide gauges prior to 1966 in our study. Continuous GPS receivers have been installed in the vicinity of both Newcastle and Port Kembla since 2010, so future studies will be able to better separate local vertical deformation effects from the records of relative sea level being collected at these tide gauges.

6.4 Noise sources and implications for sea level uncertainty

The general geographic correlation we observe between the amplitude of the seasonal cycle of sea level and the level of time-correlated noise (Figs 4–6) provides evidence supporting the idea that a portion of the coloured noise enters the residual time series through our assumption of a seasonal cycle with fixed amplitude and phase. Stochastic variations in the seasonal cycle by power-law or Gauss–Markov processes can produce power spectra that resemble those generated by long-term time-correlation processes despite the modulation only occurring at an annual frequency and related harmonic(s) (Davis *et al.* 2012). Interpreting the residual signal in the time series as being produced by a single long-memory process results in an overestimation of the rate uncertainties, if this seasonal modulation process is most important (Davis *et al.* 2012). If the departures from the average seasonal cycle tend to be a similar relative fraction of the total amplitude around the entire coastline, this process will contribute a much greater magnitude of time-correlated noise to the tide gauge records in northern Australia, where the seasonal variation is much more energetic.

In contrast to the geodetic measurements of crustal movement that have been the focus of much of the research into the effects of time-correlated noise in time series, there are well-known quasi-periodic cycles that affect sea level time series at interannual and decadal periods including El Niño/Southern Oscillation and the Pacific Decadal Oscillation (e.g. Feng *et al.* 2004). Longer term sea level variations from these oceanic processes clearly impact the estimation of the underlying rate of sea level change beyond the impacts of variation in annual periodic signals (Zhang & Church 2012). There are higher uncertainties and levels of time-correlated noise for tide gauges in southwestern Australia compared to records from the northeastern coast (Fig. 5) despite the ranges of the seasonal cycles being similar in both areas (Fig. 4). Clearly, differing levels and patterns of oceanic noise enter the tide gauge time series in different regions, making the problem of separating long-term trends from quasi-periodic signals particularly difficult. Furthermore, as noted in Introduction, the tide gauge data may include significant lags and interactions between processes described by climatic indices. Additionally, there are likely correlations between the modulation of the seasonal cycle and the lower frequency signals. Stochastic estimation of changes in seasonal cycle parameters and longer-term rates holds potential promise for determining more accurate sea level rates and uncertainties. Given the complications, we feel our conservative approach of interpreting the departures from a simple linear model as the noise component is appropriate at this time.

7 CONCLUSIONS

We have analysed tide gauge data to provide a current view of the pattern of ongoing sea level rise around continental Australia. When the noise structures of the time series of relative water levels are taken into account, only the two century-scale tide gauge records yield uncertainties on the rate of sea level rise at the 0.2 mm yr^{-1} level or better. However, by taking advantage of the high precision of differenced time series for the many pairs of tide gauges that ring the Australian coastline, we are able to estimate much higher precision estimates of the rate of relative sea level change at the shorter duration sites. Propagating the uncertainties from the adjustment, we find the average rate of sea level rise around Australia since 1900 to be 1.4 $\pm$ 0.6 mm yr^{-1} for the network of 43 tide gauges, with the highest rates ($\sim$3–5 mm yr^{-1}) occurring in northern Australia, and the lowest rates ($\sim$0–2 mm yr^{-1}) along the southern coast. The pattern is similar for the analysis over the period 1966–2011, with the mean rate shifted to 1.7 $\pm$ 0.6 mm yr^{-1}, consistent with an accelerating rate of sea level rise and other global analyses of mean sea level change. Although our adjustment process minimizes the effects of long-period ocean signals on the estimation of century-scale linear rates, it is possible that the record lengths are still too short to accurately define rates of relative sea level rates at many of the tide gauges, even with the enhanced resolution of our least-squares adjustment strategy. This may be particularly true along the tropical north coast, where the seasonal cycle is most energetic and the residual time series have the strongest temporal correlation.

Analysis of the 12 GPS–tide gauge pairs where we have adequate vertical deformation rates from GPS and relative sea level rates suggests the majority of tide gauges are recording geocentric sea level rise at the current accuracy/precision level of our measurement systems. The most anomalous tide gauge rates (particularly the Hillarys tide gauge near Perth) correlate with GPS observations of significant rates of crustal subsidence. This observation suggests that much of the local variability around the mean rates may be due to other currently unmeasured instabilities of tide gauges and benchmarks, or broader crustal deformation. Our observations underscore the importance of maintaining a dense network of long-term tide gauges that measure water levels against stable and consistent datums, and the need to continue co-location of continuous GNSS receivers and high-quality tide gauges.

ACKNOWLEDGEMENTS

This project was supported under the Australian Research Council's Discovery Projects funding scheme (DP0877381). We thank the Australian National Tidal Centre and the Permanent Service for Mean Sea Level for making the tide gauge observations available. We acknowledge the International GNSS Service for distributing the raw GPS data. We are grateful to Simon Williams for creating and sharing the CATS program and providing important clarifications and insights. We thank Alvaro Santamaría-Gómez, Matt Chamberlain and an anonymous reviewer for constructive reviews that improved the clarity and accuracy of the manuscript. Map figures were made with the Generic Mapping Tools software (Wessel & Smith 1991).

REFERENCES

Agnew, D.C., 1992. The time-domain behavior of power-law noises, *Geophys. Res. Lett.,* **19**(4), 333–336.

Altamimi, Z., Collilieux, X. & Metivier, L., 2011. ITRF2008: an improved solution of the international terrestrial reference frame, *J. Geodyn.,* **85,** 457–473.

Ananga, N., Coleman, R. & Rizos, C., 1995. Geodetic monitoring of tide gauge bench marks with GPS, *J. Geodetic Soc. Japan,* **41,** 91–97.

Aubrey, D.G. & Emery, K.O., 1986. Australia—an unstable platform for tide-gauge measurements of changing sea levels, *J. Geol.,* **94,** 699–712.

Belperio, A.P., 1993. Land subsidence and sea level rise in the Port Adelaide estuary: implications for monitoring the greenhouse effect, *Aust. J. Earth Sci.,* **40,** 359–368.

Bevis, M., Scherer, W. & Merrifield, M., 2002. Technical issues and recommendations related to the installation of continuous GPS stations at tide gauges, *Mar. Geod.,* **25,** 87–99.

Bekesi, G., McGuire, M. & Moiler, D., 2009. Groundwater allocation using a groundwater level response management method—Gnangara groundwater system, Western Australia, *Water Resour. Manage.,* **23**,1665–1683.

Bindoff, N.L. *et al.*, 2007. Observations: oceanic climate change and sea level, in *Climate Change 2007: The Physical Science Basis. Contribution of Working Group I to the Fourth Assessment Report of the Intergovernmental Panel on Climate Change,* eds Solomon, S., Qin, D., Manning, M., Chen, Z., Marquis, M., Averyt, K.B., Tignor, M. & Miller, H.L., Cambridge University Press, Cambridge, United Kingdom, and New York, NY, USA.

Bouin, M.N. & Woppelmann, G., 2010. Land motion estimates from GPS at tide gauges: a geophysical evaluation, *Geophys. J. Int.,* **180,** 193–209.

Burgette, R.J., Weldon, R.J. & Schmidt, D.A., 2009. Interseismic uplift rates for western Oregon and along-strike variation in locking on the Cascadia subduction zone, *J. geophys. Res.,* **114,** B01408, doi:10.1029/2008JB005679.

Chambers, D.P., Merrifield, M.A. & Nerem, R.S., 2012. Is there a 60-year oscillation in global mean sea level? *Geophys. Res. Lett.,* **39,** L18607, doi:10.1029/2012GL052885.

Chen, K. & McAneney, J., 2006. High-resolution estimates of Australia's coastal population, *Geophys. Res. Lett.,* **33,** L16601, doi:10.1029/2006GL026981.

Church, J.A. & White, N.J., 2011. Sea-level rise from the late 19th to the early 21st century, *Surv. Geophys.,* **32,** 585–602.

Church, J.A., Hunter, J.R., McInnes, K.L. & White, N.J., 2006. Sea level rise around the Australian coastline and the changing frequency of extreme sea-level events, *Aust. Met. Mag.,* **55,** 253–260.

Church, J.A., White, N.J., Coleman, R., Lambeck, K. & Mitrovica, J.X., 2004. Estimates of the regional distribution of sea level rise over the 1950–2000 period, *J. Clim.,* **17,** 2609–2625.

Church, J.A. *et al.*, 2011. Revisiting the Earth's sea-level and energy budgets from 1961 to 2008, *Geophys. Res. Lett.,* **38,** L18601, doi:10.1029/2011GL048794.

Coleman, R. *et al.*, 2008. New geodetic infrastructure for Australia, *J. Spat. Sci.,* **53**(2), 65–80.

Davis, J.L., Wernicke, B.P. & Tamisiea, M.E., 2012. On seasonal signals in geodetic time series, *J. geophys. Res.,* **117,** B01403, doi:10.1029/2011JB008690 .

Douglas, B.C., 1991. Global sea level rise, *J. geophys. Res.,* **96**(C4), 6981–6992.

Featherstone, W.E., Filmer, M.S., Penna, N.T., Morgan, L.M. & Schenk, A., 2012. Anthropogenic land subsidence in the Perth Basin: challenges for its retrospective geodetic detection, *J. R. Soc. West. Aust.,* **95,** 53–62.

Feng, M., Li, Y. & Meyers, G., 2004. Multidecadal variations of Fremantle sea level: footprint of climate variability in the tropical Pacific, *Geophys. Res. Lett.,* **31,** L16302, doi:10.1029/2004GL019947.

Fleming, K.M, Tregoning, P., Kuhn, M., Purcell, A. & McQueen, H., 2012. The effect of melting land-based ice masses on sea-level around the Australian coastline, *Aust. J. Earth Sci.,* **59,** 457–467.

Forbes, A.M.G. & Church, J.A., 1983. Circulation in the Gulf of Carpentaria II: residual currents and mean sea level, *Aust. J. Mar. Freshw. Res.,* **34,** 1–10.

Gregory, J.M. *et al.*, 2013. Twentieth-century global-mean sea-level rise: is the whole greater than the sum of the parts? *J. Clim.,* doi:10.1175/JCLI-D-12-00319.1.

Herring, T.A., King, R.W. & McClusky, S., 2008. *Introduction to GAMIT/GLOBK,* Massachusetts Institute of Technology, Cambridge.

Holbrook, N.J., Goodwin, I.D., McGregor, S., Molina, E. & Power, S.B., 2011. ENSO to multi-decadal time scale changes in East Australian Current transports and Fort Denison sea level: Oceanic Rossby waves as the connecting mechanism, *Deep Sea Res. II: Topical Stud. Oceanogr.,* **58,** 547–558.

Hughes, C.W. & Williams, S.D.P., 2010. The color of sea level: importance of spatial variations in spectral shape for assessing the significance of trends, *J. geophys. Res.,* **115,** C10048, doi:10.1029/2010JC006102.

Jevrejeva, S., Grinsted, A., Moore, J.C. & Holgate, S., 2006. Nonlinear trends and multiyear cycles in sea level records, *J. geophys. Res.,* **111,** C09012, doi:10.1029/2005JC003229.

King, M.A., Keshin, M., Whitehouse, P.L., Thomas, I.D., Milne, M. & Riva, R.E., 2012. Regional biases in absolute sea-level estimates from tide gauge data due to residual unmodeled vertical land movement, *Geophys. Res. Lett.,* **39,** L14604, doi:10.1029/2012GL052348.

Lambeck, K., 2002. Sea-level change from mid-Holocene to recent time: an Australian example with global implications, in, *in Ice Sheets, Sea Level and the Dynamic Earth,* eds Mitrovica, J.X. & Vermeersen, B.L.A., *Geodyn. Ser.,* Vol. 29, AGU, Washington, DC, USA, pp. 33–50.

Langbein, J., 2004. Noise in two-color electronic distance meter measurements revisited, *J. geophys. Res.,* **109,** B04406, doi:10.1029/2003JB002819.

Langbein, J. & Johnson, H., 1997. Correlated errors in geodetic time series: implications for time-dependent deformation, *J. geophys. Res.,* **102**(B1), 591–603.

Mandelbrot, B.B. & Van Ness, J.W., 1968. Fractional Brownian motions, fractional noises, and applications, *SIAM Rev.,* **10**(4), 422–437.

Maul, G.A. & Martin, D.M., 1993. Sea level rise at Key West, Florida, 1846–1992: America's longest instrument record? *Geophys. Res. Lett.,* **20,** 1955–1958.

Mazzotti, S., Jones, C. & Thomson, R.E., 2008. Relative and absolute sea level rise in western Canada and northwestern United States from a combined tide gauge-GPS analysis, *J. geophys. Res.,* **113,** C11019, doi:10.1029/2008JC004835.

Milne, G.A., Davis, J.L., Mitrovica, J.X., Scherneck, H.G., Johansson, J.M., Vermeer, M. & Koivula, H., 2001. Space-geodetic constraints on glacial isostatic adjustment in Fennoscandia, *Science,* **291,** 2381–2385.

Montgomery, D., Peck, E. & Vining, G., 2006. *Introduction to Linear Regression Analysis,* 4th edn, pp. 640, John Wiley and Sons, Hoboken, NJ, USA.

Nerem, R.S. & Mitchum, G.T., 2001. Observations of sea level change from satellite altimetry, in *Sea Level Rise: History and Consequences,* eds Douglas, B.C., Kearney, M.S. & Leatherman, S.P., *Int. Geophys. Ser.,* Vol. 75, pp. 121–163. Academic Press, San Diego, CA, USA.

NTC, 2011. *The Australian Baseline Sea Level Monitoring Project annual sea level data summary report July 2010–2011,* pp. 41, Kent Town, SA.

Santamaría-Gómez, A., Bouin, M.N., Collilieux, X. & Woppelmann, G., 2011. Correlated errors in GPS position time series: implications for velocity estimates, *J. geophys. Res.,* **116,** B01405, doi:10.1029/2010JB007701.

Santamaría-Gómez, A., Gravelle, M., Collilieux, X., Guichard, M., Martín Míguez, B., Tiphaneau, P. & Wöppelmann, G., 2012. Mitigating the effects of vertical land motion in tide gauge records using a state-of-the-art GPS velocity field, *Global planet. Change,* **98–99,** 6–17.

Tregoning, P. & Watson, C., 2009. Atmospheric effects and spurious signals in GPS analyses, *J. geophys. Res.,* **114,** B09403, doi:10.1029/2009JB006344.

Tregoning, P., Morgan, P.J. & Coleman, R., 2004. The effect of receiver firmware upgrades on GPS vertical timeseries, *Cahiers du Centre Eur. Géodyn. Séismol.,* **23,** 37–46.

Tregoning, P., Watson, C., Ramillien, G., McQueen, H. & Zhang, J., 2009. Detecting hydrologic deformation using GRACE and GPS, *Geophys. Res. Lett.,* **36,** L15401, doi:10.1029/2009GL038718.

Tregoning, P., Burgette, R., McClusky, S.C., Lejeune, S., Watson, C.S. & McQueen, H., 2013. A decade of horizontal deformation from great earthquakes. *J. geophys. Res.,* doi:10.1002/jgrb.50154.

Watson, P.J., 2011. Is there evidence yet of acceleration in mean sea level rise around mainland Australia? *J. Coastal Res.,* **27**(2), 368–377.

Wessel, P. & Smith, W.H.F., 1991. Free software helps map and display data, *EOS, Trans. Am. geophys. Un.,* **72,** 441–446.

Williams, S.D.P., 2003. The effect of coloured noise on the uncertainties of rates estimated from geodetic time series, *J. Geodyn.,* **76,** 483–494.

Williams, S.D.P., 2008. CATS: GPS coordinate time series analysis software, *GPS Solut.,* **12,** 147–153.

Williams, S.D.P., Bock, Y., Fang, P., Jamason, P., Nikolaidis, R.M., Prawirodirdjo, L., Miller, M. & Johnson, D.J., 2004. Error analysis of continuous GPS position time series, *J. geophys. Res.,* **109,** B03412, doi:10.1029/2003JB002741.

Williams, S.D.P. & Willis, P., 2006. Error analysis of weekly station coordinates in the DORIS network, *J. Geodyn.,* **80,** 525–539.

Woodworth, P.L. & Player, R., 2003. The permanent service for mean sea level: An update to the 21st century, *J. Coastal Res.,* **19,** 287–295.

Woodworth, P.L., Tsimplis, M.N., Flather, R.A. & Shennan, I., 1999. A review of the trends observed in British Isles mean sea level data measured by tide gauges, *Geophys. J. Int.,* **136,** 651–670.

Woodworth, P.L., Teferle, F.N., Bingley, R.M., Shennan, I. & Williams, S.D.P., 2009a. Trends in UK mean sea level revisited, *Geophys. J. Int.,* **176,** 19–30.

Woodworth, P.L., White, N.J., Jevrejeva, S., Holgate, S.J., Church, J.A. & Gehrels, W.R., 2009b. Evidence for the accelerations of sea level on multi-decade and century timescales, *Int. J. Clim.,* **29,** 777–789.

Woppelmann, G., Letetrel, C., Santamaria, A., Bouin, M.N., Collilieux, X., Altamimi, Z., Williams, S.D.P. & Martin Miguez, B., 2009. Rates of sea-level change over the past century in a geocentric reference frame, *Geophys. Res. Lett.,* **36,** L12607, doi:10.1029/2009GL038720.

Zhang, J., Bock, Y., Johnson, H., Fang, P., Williams, S., Genrich, J., Wdowinski, S. & Behr, J., 1997. Southern California Permanent GPS Geodetic Array: error analysis of daily position estimates and site velocities, *J. geophys. Res,* **102**(B8), 18 035–18 055.

Zhang, X. & Church, J.A., 2012. Sea level trends, interannual and decadal variability in the Pacific Ocean, *Geophys. Res. Lett.,* **39,** L21701, doi:10.1029/2012GL053240.

APPENDIX A: LEAST-SQUARES ADJUSTMENT METHOD

Our adjustment technique estimates the adjusted rate of relative sea level rise, RSL_i^{Adj}, at each tide gauge, i, in the network using two types of observation equations and a solution through the method of generalized least squares (Fig. 2a, black lines). First, for each tide gauge with observations over the full analysis time period, we use individual time series and CATS software (Williams 2008) to calculate the rate and associated uncertainty, RSL_i^{CATS} and σ_i^{CATS} (Fig. 2a, blue lines for sites with black labels). Second, we difference time series from specific pairs of tide gauges i and j, and estimate using CATS the differential rates of relative sea level change and associated uncertainty, Δ_{ij}^{CATS} and $\sigma\Delta_{ij}^{CATS}$ (Fig. 2b, blue lines). Each differential rate is estimated using data from common epochs for gauges i and j, within the temporal window of the analysis. For each tide gauge, i, in the complete network, we include in the adjustment the four values of Δ_{ij}^{CATS} with the lowest uncertainties, $\sigma\Delta_{ij}^{CATS}$, selected from i's geographically nearest 10 neighbours. We ensure that any given differential rate is used only once (i.e. if Δ_{ab}^{CATS} is used, Δ_{ba}^{CATS} is not).

These two types of observations yield two primary observation equations,

$$RSL_i^{Adj} - RSL_i^{CATS} = v_i \tag{A1}$$

and

$$RSL_i^{Adj} - RSL_j^{Adj} - \Delta_{ij}^{CATS} = v_{ij}, \tag{A2}$$

where v_i and v_{ij} are the residuals related to each observation.

For tide gauges with records that span the entire analysis time period, we use both observation types (RSL_i^{CATS} and Δ_{ij}^{CATS}; eqs A1 and A2), whereas tide gauges with shorter durations only enter the adjustment in terms of the differential rates (Δ_{ij}^{CATS}), as per eq. A2 only. We solve the system of equations for each temporal analysis window using the matrix solution for generalized least squares.

We construct a fully populated variance-covariance matrix, $\mathbf{W}$, using the CATS uncertainty estimates associated with the linear rates (treated as observations in the adjustment) to calculate the observation variance entries of $\mathbf{W}$ for each observation, p, W_{pp}. Our strategy of analysing individual time series using CATS does not provide direct estimates of the covariances between the rate estimates (from individual and differenced time series) for input into the $\mathbf{W}$ matrix in the adjustment. As the uncertainty of the estimates depends upon the residual noise structure of each time series, we use correlations between residual time series to approximate the off-diagonal terms of this matrix in a pairwise fashion (between all observation pairs p and q of RSL_i^{CATS} and Δ_{ij}^{CATS}). We calculate the dimensionless correlation coefficient R_{pq} for each pair of residual time series. In determining the correlation coefficient, we normalize by the number of monthly observations in the union of the two time series being compared, as observations missing from one time series de-correlate the estimated rates. We estimate the covariances as $W_{\mathrm{pq}} = R_{\mathrm{pq}}\ (W_{\mathrm{pp}} * W_{\mathrm{qq}})^{0.5}$.

In a network of n stations with m total observations (comprising both individual site rates and intersite differential rates), $\mathbf{L}$ is an $m \times 1$ vector of observed values of RSL_i^{CATS} and Δ_{ij}^{CATS}, $\mathbf{A}$ is an m by n matrix of partial derivatives from the observation equations A1 and A2 relating the observations in $\mathbf{L}$ to the adjusted rate parameters, RSL_i^{Adj}, $\mathbf{W}$ is an m by m matrix of variances and covariances corresponding to the observations in $\mathbf{L}$, $\mathbf{X}$ is the $n \times 1$ vector of best-fit parameters (RSL_i^{Adj}; see Fig. 2a, black lines for all sites) and $\mathbf{V}$ is an $m \times 1$ vector of residuals (v_i and v_{ij}), that is, $\mathbf{V} = \mathbf{A}*\mathbf{X} - \mathbf{L}$. For all three analysis periods of this study, $n = 43$, and $m = 117$, 129 and 156, for the periods beginning in 1900, 1966 and 1993, respectively.

We use least squares to solve this over-determined set of equations, minimizing the quantity $\mathbf{V}^{\mathrm{T}} * \mathbf{W}^{-1} * \mathbf{V}$. The off-diagonal terms in $\mathbf{W}$ require the use of generalized least squares (Montgomery *et al.* 2006), with the solution

$$\mathbf{X} = \left(\mathbf{A}^{\mathrm{T}} * \mathbf{W}^{-1} * \mathbf{A}\right)^{-1} * \mathbf{A}^{\mathrm{T}} * \mathbf{W}^{-1} * \mathbf{L}. \tag{A3}$$

The mean squared error of the adjustment is

$$M = \mathbf{L}^{\mathrm{T}} * \left(\mathbf{W}^{-1} - \mathbf{W}^{-1} * \mathbf{A} * \left(\mathbf{A}^{\mathrm{T}} * \mathbf{W}^{-1} * \mathbf{A}\right)^{-1} * \mathbf{A}^{\mathrm{T}} * \mathbf{W}^{-1}\right) * \mathbf{L}/(m - n), \tag{A4}$$

and the estimated output variance-covariance matrix is

$$\mathbf{S} = \left(\mathbf{A}^{\mathrm{T}} * \mathbf{W}^{-1} * \mathbf{A}\right)^{-1} * M, \tag{A5}$$

from which we obtain the uncertainties of the adjusted rates of relative sea level rise, σ_i^{Adj}, for each tide gauge in the analysis.

SUPPORTING INFORMATION

Additional Supporting Information may be found in the online version of this article:

Table S1. Candidate tide gauge records from the Permanent Service for Mean Sea Level (PSMSL) excluded from the analysis due to suspected datum instability and other temporal anomalies in time series.

Table S2. Anomalous portions of monthly tide gauge data at the beginning and/or end of time series excluded from time-series analysis. See Table 1 for site codes and locations. (http://gji.oxfordjournals.org/lookup/suppl/doi:10.1093/gji/ggt131/-/DC1)

Please note: Oxford University Press is not responsible for the content or functionality of any supporting materials supplied by the authors. Any queries (other than missing material) should be directed to the corresponding author for the article.